DOT/FAA/AR-05/5,I

Development and Validation of an Aircraft Seat Cushion Component Test—Volume I

March 2005

Final Report

This document is available to the public through the National Technical Information Service (NTIS), Springfield, Virginia 22161.

U.S. Department of Transportation
Federal Aviation Administration

NOTICE

This document is disseminated under the sponsorship of the U.S. Department of Transportation in the interest of information exchange. The United States Government assumes no liability for the contents or use thereof. The United States Government does not endorse products or manufacturers. Trade or manufacturer's names appear herein solely because they are considered essential to the objective of this report. This document does not constitute FAA certification policy. Consult your local FAA aircraft certification office as to its use.

This report is available at the Federal Aviation Administration William J. Hughes Technical Center's Full-Text Technical Reports page: actlibrary.tc.faa.gov in Adobe Acrobat portable document format (PDF).

Technical Report Documentation Page

1. Report No. DOT/FAA/AR-05/5,I	2. Government Accession No.	3. Recipient's Catalog No.
4. Title and Subtitle DEVELOPMENT AND VALIDATION OF AN AIRCRAFT SEAT CUSHION COMPONENT TEST—VOLUME I		5. Report Date March 2005
		6. Performing Organization Code
7. Author(s) S.J. Hooper and M.J. Henderson		8. Performing Organization Report No.
9. Performing Organization Name and Address J.B. Dwerlkotte Assoc., Inc. 429 N. St. Francis Wichita, KS 67202		10. Work Unit No. (TRAIS)
		11. Contract or Grant No.
12. Sponsoring Agency Name and Address U.S. Department of Transportation Federal Aviation Administration Office of Aviation Research Washington, DC 20591		13. Type of Report and Period Covered
		14. Sponsoring Agency Code ANM-102N
15. Supplementary Notes The FAA William J. Hughes Technical Center COTR was Mr. Timothy G. Smith. The work was performed under subcontract to The National Institute for Aviation Research at Wichita State University, Wichita, KS 67260.		

16. Abstract

A component test method was developed and validated to certify replacement bottom seat cushions for 16-g aircraft seats that were originally certified to the requirements of Title 14 Code of Federal Regulations 25.562 or Technical Standard Order C127a. The methodology established criteria to evaluate replacement cushions, which ensures an equivalent or improved level of safety to the cushions originally certified on these seats. The component test was derived from American Society for Testing and Materials standard test method D 3574-03 and generates load-deflection data for a cylindrical test specimen. The component test method was validated, using test results produced during full-scale 14-g sled tests performed at the Federal Aviation Administration Civil Aerospace Medical Institute.

17. Key Words 16-g seat, Lumbar load, Cushion properties		18. Distribution Statement This document is available to the public through the National Technical Information Service (NTIS) Springfield, Virginia 22161.	
19. Security Classif. (of this report) Unclassified	20. Security Classif. (of this page) Unclassified	21. No. of Pages 77	22. Price

Form DOT F 1700.7 (8-72)   Reproduction of completed page authorized

ACKNOWLEDGEMENTS

TABLE OF CONTENTS

LIST OF FIGURES

LIST OF TABLES

LIST OF ACRONYMS

AGATE	Advanced General Aviation Technology Experiments
AS	SAE Aerospace Standard
ASTM	American Society of Testing and Materials
ATD	Anthropomorphic test dummy
BRP	Buttock reference point
CAMI	Civil Aerospace Medical Institute
CFR	Code of Federal Regulations
DRI	Dynamic response index
FAA	Federal Aviation Administration
g	Acceleration of gravity (32.2 ft/sec^2)
IFD	Indentation Force Deflection (lb)
MPT	Multipurpose Testware
SRP	Seat reference point
TSO	Technical Standard Order

EXECUTIVE SUMMARY

This report describes the methodology that was employed to develop and verify the pass-fail criteria associated with the aircraft Seat Cushion Component Test. This component test provides a pass-fail criterion based on an "equivalent or improved level of safety" and will be used in comparative tests of the certified bottom seat cushion and a candidate replacement cushion. The successful component test of a candidate replacement bottom seat cushion shows that its design satisfies the applicable lumbar load injury criterion specified in Title 14 Code of Federal Regulations 25.562 or Technical Standard Order C127a.

1. INTRODUCTION.

1.1 PURPOSE.

The research documented in this report was conducted to develop and validate a component test method that can be used to show compliance with the lumbar load injury criterion specified in Title 14 Code of Federal Regulations (CFR) 25.562 for replacement aircraft bottom seat cushions.

1.2 BACKGROUND.

The properties of aircraft bottom seat cushions are known to have a strong influence on the lumbar load performance of 16-g (acceleration of gravity) dynamically certified aircraft passenger seats. Aircraft seat cushions must be periodically replaced due to wear and abuse during normal service. Most airlines acquire replacement cushions that are identical to those originally certified by the seat supplier. However, operators cannot count on the availability of identical cushions since the foam materials used in the cushion fabrication may no longer be produced. If this is the case, operators are required to conduct full-scale dynamic seat tests, illustrated in figure 1-1 for the purpose of certifying a replacement cushion. This has motivated industry and the Federal Aviation Administration (FAA) to develop a suitable component seat cushion test as an alternative method to certify replacement bottom seat cushions.

The current regulations, i.e., the emergency landing dynamic conditions (14 CFR 25.562(c)(2)) [1], require that seat designs satisfy the requirements in vertical and horizontal test conditions. The lumbar load injury criterion is generally critical for the vertical test conditions of 14 CFR 25.562(b)(1) and, thus, is the subject of in this report. Full-scale dynamic seat testing, per 14 CFR 25.562(b)(1), requires a specific minimum velocity, minimum acceleration, and maximum rise time, as listed in table 1-1. These requirements are also required by Technical Standard Order (TSO) C127a [2].
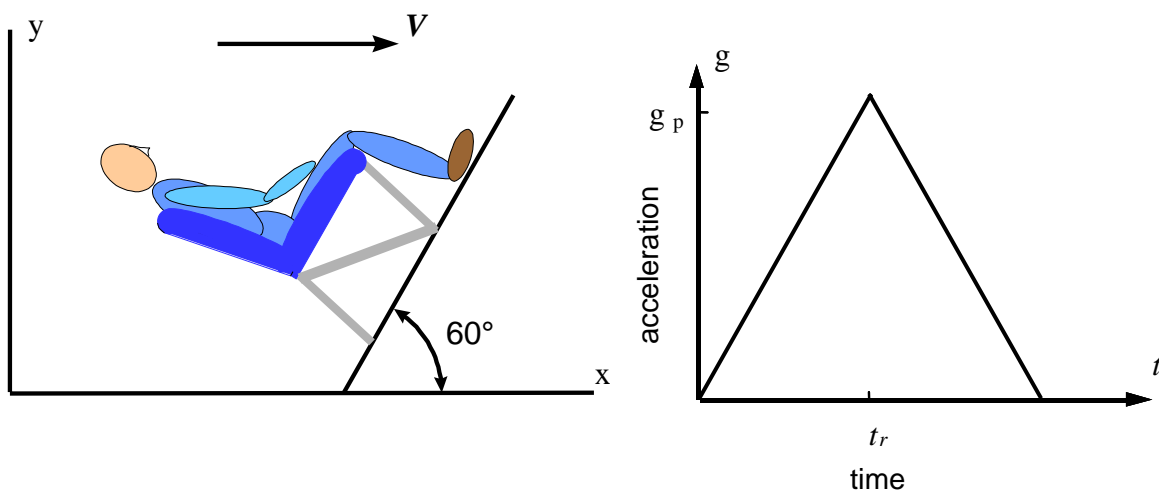
FIGURE 1-1. FOURTEEN-g DYNAMIC SLED TEST CONDITIONS

1-1

TABLE 1-1. FOURTEEN-g IMPULSE DEFINITION

Velocity Change	ΔV	ft/sec	35
Peak Acceleration	g_p	g's	14
Rise Time	t_r	sec	0.080

Stech and Payne were among the first to address the spinal injury problem for aircraft seats when they developed a spring-mass model to predict an occupant response during ejection seat testing [3]. This model represented the biodynamic properties of the human body and suggested a spinal injury mechanism that is especially sensitive to the spring force in the spinal column. This injury mechanism has become known as the Dynamic Response Index (DRI) and is currently used by the Department of Defense as a criterion with which to evaluate the performance of ejection seats [4]. While the DRI measure is appropriate for the relatively stiff ejection seats installed in military aircraft, its application to civil aircraft seats has produced unrealistic results [5]. Subsequent research, at the FAA Civil Aerospace Medical Institute (CAMI) [6], led to the development of the 1500-lb spinal injury criterion contained in 14 CFR 25.562 and TSO-C127a. The spinal injury criterion was developed using a modified 49 CFR Part 572, support B anthropomorphic dummy, which continues to be used in dynamic seat tests. The dummy modifications are described in SAE International Aerospace Standard (AS) 8049 Rev(A) [7]. The 1500-lb load limit corresponds to a DRI of about 19. Data for the military population at that time indicate that the probability of detectable spinal injury at DRI = 18 is about 5 percent and about 20 percent at a DRI of 22. Thus, a DRI of 19 corresponds to a probability of spinal injury of about 9 percent.

Other researchers developed a number of occupant models to investigate spinal injuries for ejection seats and crashworthy seat designs. These initially included a number of lumped parameter models [8 and 9] as well as the commonly known SOM-LA and MADYMO computer programs described in references 10 and 11. Many of these early models [10 and 12] simplified the seat cushion behavior by representing the relationship between cushion force and displacement with a simple exponential function.

$$F = C[e^{B\delta} - 1] \tag{1-1}$$

where F and δ represent the cushion force and displacement, respectively, and B and C are material properties. This function is plotted in figure 1-2, where it is seen that the cushion force asymptotically approaches zero as the displacement approaches zero.

The load-deflection curve reflects the common perception regarding cushion behavior, and it is commonly used in biodynamic simulations. The problem is that cushion data attracts attention to that portion of the curve with the greatest load and displacement. Unfortunately, if one selects a load cell to measure the highest load, it cannot accurately measure the lower load levels.
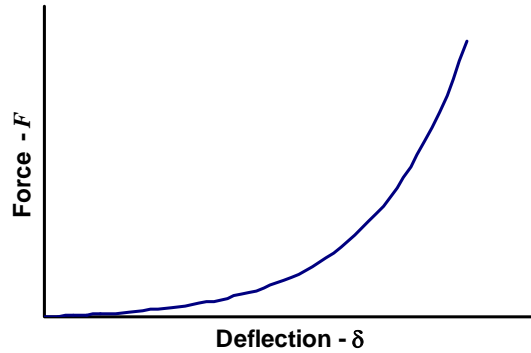
FIGURE 1-2. EXPONENTIAL LOAD-DEFLECTION CURVE

The furniture industry has traditionally used the Indentation Force Deflection (IFD) test to characterize foam materials. The IFD is defined in American Society of Testing and Materials (ASTM) standard test method B_1 method D 3574-03 [13] and is commonly used by the aircraft seating industry. The forces are recorded at 25% and 65% of the cushion thickness during static tests that are typically performed using screw-driven material test stands.

Gibson and Ashby [14] published a comprehensive text on cellular solids in 1997 in which they identify typical load-deflection curves, as shown in figure 1-3. The functional form of these curves possesses three distinct regions: the initial linear elastic region, the plateau region (which may show some increase in strength as the deformation increases such as shown in figure 1-3(b)), and the densification region.

(a)   (b)
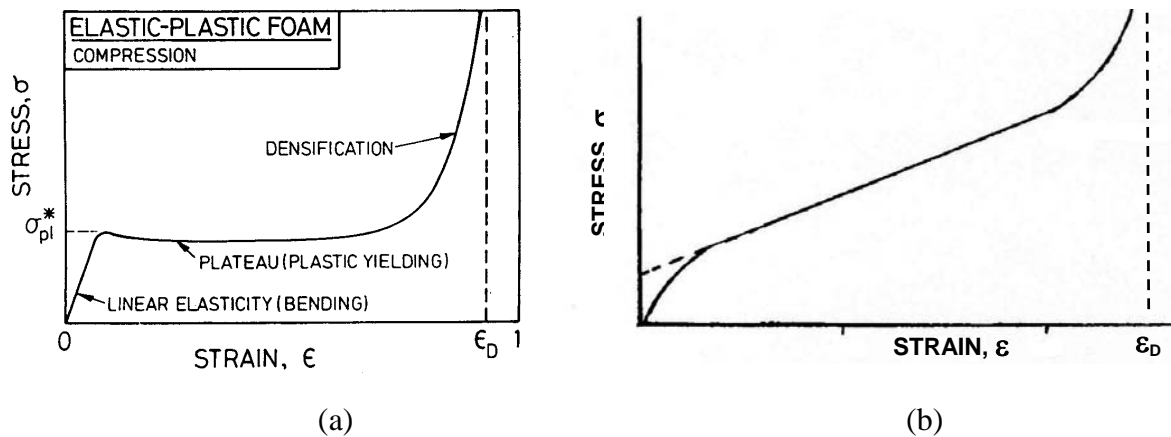
FIGURE 1-3. TYPICAL STRESS-STRAIN BEHAVIOR OF CELLULAR SOLIDS

The densification strain, ε_D, is defined as the strain where the stress approaches a vertical asymptote. The linear elastic region is generally very small for the foam materials used in furniture and seat cushions. The plateau strength region spans most of the stress strain curve along the strain axis, and the densification region is limited to a relatively small portion of the strain axis where the highest stresses occur.

1-3

It should be noted that IFD data are simply two points in the plateau region. Early dynamic seat researchers did not recognize the significance of the plateau strength, in part because they were focused on ejection seat performance, and the cushions in the early ejection seats were not constructed of the same kinds of materials as cushions used in transport aircraft seats. Early studies by Payne and others simply concluded that seat cushions tended to amplify the lumbar load, an effect that is minimized by increasing the firmness of the seat cushion. In retrospect, the importance of the plateau strength should have been suspected when the importance of the 1-g dummy preload was recognized and new dynamic seat test procedures developed and incorporated into AS8049 Rev(A) and Advisory Circular 25.562 Rev 1A [7 and 15].

It is appropriate to review the definitions of stress and strain prior to presenting the results of this research. Engineering strain is defined as

$$\bar{e} = \lim_{\Delta x \to 0} \frac{\Delta \bar{u}}{\Delta \bar{x}} = \frac{d\,\bar{u}}{d\,\bar{x}} \tag{1-2}$$

which is commonly expressed as

$$\bar{e} = \frac{\Delta \bar{\ell}}{\ell_0} \quad \text{where} \quad \frac{\Delta \bar{\ell}}{\ell_0} \ll 1 \tag{1-3}$$

where ℓ_0 represents the initial unloaded specimen length and $\Delta \bar{\ell}$ represents the change in its length. Clearly, the material performance presented in figure 1-3 involves strains whose magnitude approaches unity. Therefore, it is necessary to employ an appropriate definition of strain. The logarithmic, or true, strain and the Green-Lagrange strain [16 and 17] represent two appropriate possibilities. The logarithmic, or true, strain is employed in the following analysis and is defined as

$$d\bar{\varepsilon} = \frac{d\bar{\ell}}{\ell} \tag{1-4}$$

which upon integration gives

$$\bar{\varepsilon} = \ln\left(\frac{\ell}{\ell_0}\right) = \ln\left(1 + \bar{e}\right) \tag{1-5}$$

Foam materials possess limited tensile strength and are nearly always loaded in compression. The common convention is to characterize foam properties in terms of compressive strength and strain, which are both presented as positive quantities. The above equations are easily transformed to this coordinate system, which results in the following expressions for engineering strain and logarithmic strain.

$$e = \frac{-\Delta\ell}{\ell_0} \quad \text{where} \quad \left|\frac{-\Delta\ell}{\ell_0}\right| \ll 1 \tag{1-6}$$

where ℓ_0 represents the initial unloaded length and $-\Delta\ell$ represents the shortening of its length. The corresponding logarithmic, or true, strain is subsequently expressed as

$$\varepsilon = -\ln\left(\frac{\ell}{\ell_0}\right) = -\ln(1-e) \tag{1-7}$$

where positive values of e are used to represent compressive deformations. Engineering stress is defined as

$$\sigma = \lim_{\Delta A \to 0} \frac{-\Delta F}{\Delta A} = \frac{-F}{A} \tag{1-8}$$

where A represents a surface area in the unloaded geometry and F represents a force acting on this surface area. This definition also employs the convention that compressive stresses are reported as positive numbers.

The deflection and force data for a single layer of foam are calculated from stresses and strains by the following equations

$$\delta = -h\left(e^{-\varepsilon} - 1\right) \tag{1-9}$$

$$F = -\sigma A \tag{1-10}$$

where h represents the thickness of the material specimen. The force and deflection data for laminated materials subject to uniaxial loading are extracted by recognizing that the same force, F, is applied to both material layers. The displacements in the top and bottom layers, δ_1 and δ_2, can be written as

$$\delta_1 = \delta_1(F) \tag{1-11}$$

$$\delta_2 = \delta_2(F) \tag{1-12}$$

The load-deflection data generated during the materials tests were represented by a smooth sequence of straight-line segments where δ varies monotonically with F. This allows equations 1-11 and 1-12 to be evaluated by a simple linear interpolation algorithm. The total displacement of a laminated cushion is the sum of these

$$\delta = \delta_1 + \delta_2 \tag{1-13}$$

The importance of rate sensitivity has been the subject of a number of industry discussions over the past several years. Gibson and Ashby concluded that all polymeric foams exhibit rate sensitive behavior to some degree since their glass transition temperature T_G, is so close to ambient room temperature. Consequently, Hooper and Henderson developed a dynamic component test, which could be used to test the performance of cushions and diaphragms [18]. Another cushion component test was developed during the FAA/NASA Advanced General

Aviation Technology Experiments (AGATE) program [19] that employed a rate relaxation test to address the rate sensitivity issue. The AGATE method has not been validated, and the Hooper-Henderson method includes a seat pan or diaphragm as part of the test article, a requirement that many perceive as too costly and complicated.

2. RESEARCH DESCRIPTION.

This research was performed to develop and validate a component cushion test that can be used to certify bottom seat cushions for 16-g aircraft seats. One of the first issues was to determine whether typical seat cushion materials are rate sensitive or not. Material tests were performed statically and at relatively high loading rates of 30 in./sec using MTS Servohydraulic test stands. EAR CONFOR® specimens were also tested since this material is known to possess significant rate sensitivity [20].

The test fixture and methodology for the cushion component tests were adapted from the IFD method described in ASTM D 3574-03.

The test fixture and methodology for the cushion component tests were adapted from the IFD method described in ASTM D 3574-03. The component tests differed from the IFD test in following ways:

- They employed a 30-in./sec loading rate rather than a static loading rate.

- Data were collected for the complete loading and unloading curve rather than just measuring the indentation force at 25% and 65% of the unloaded cushion thickness.

Nonflotation and flotation cushion specimens were tested during the component tests. The latter were fabricated as a soft foam layer that was laminated on top of a rigid flotation foam substrate. The rigid foams are distinguished from the soft foams by the fact that they sustain permanent damage that can be detected either by a visual inspection or by carefully examining the test data. The data acquired during these tests were analyzed and used to select nonflotation and flotation cushions for lumbar load evaluation in dynamic sled tests. The flotation specimens were designed to satisfy the requirements of TSO-C72c [21]. The cushions selected for the dynamic sled test program represented the strongest, weakest, and those exhibiting intermediate strength properties.

The lumbar loads of selected cushions were evaluated with an anthropomorphic test dummy during dynamic sled tests performed per 14 CFR 25.562(b)(1) at the FAA CAMI laboratory in Oklahoma City. A rigid seat was used during these tests. The results are shown in appendix A.

2.1 TEST SETUP.

The dynamic component tests were performed in the Wichita State University Composites Laboratory using a 220-kip MTS load frame (see figure 2-1) equipped with a 110-kip servohydraulic actuator and instrumented with two load cells: a conventional 150-kip strain gage-type load cell and a 10-kip piezoresistive load cell. This load frame is fitted with a 180-GPM servovalve and a large oil accumulator bank. This configuration enables the machine to displace large amounts of oil at very high speeds, thus generating very high loading rates. The dynamic testing was performed at a loading rate of 30 in./sec. The static tests were conducted

---

® Registered trademark licensed to the AERO Company.

using a conventional 22-kip servohydraulic MTS load frame at a loading rate of 0.033 in./sec. The rate sensitivity of a cushion can be determined by comparing the static and dynamic test results. These results will be nearly identical for non-rate-sensitive materials, and they will differ significantly for rate-sensitive materials.

FIGURE 2-1. MTS 220-kip DYNAMIC LOAD FRAME

The MTS test equipment was calibrated and verified according to ASTM E 4 to ensure the accuracy of the applied loads and displacements. After calibration, the MTS machine was tuned to ensure that the load and displacement feedbacks follow, as closely as possible, the corresponding command.

The material is specified as either 2024-T351 or 7075-T651 aluminum. All fillet radii are specified as 1/4 in. The platen was perforated per ASTM D 3574-03 with 1/4-in. holes on 3/4-in. centers (approximately) as shown in figure 2-2. These holes allow the trapped air in the cushion material to escape during the test. The close-up view of the test setup is shown in figure 2-3 and shows the conventional strain gage-type load cell and the piezoresistive load cell as well as the 8-in.-diameter foot used to load the specimens. The foot was bolted to an MTS hemispherical platen, which was attached to the actuator.

FIGURE 2-2. PLATEN DESIGN
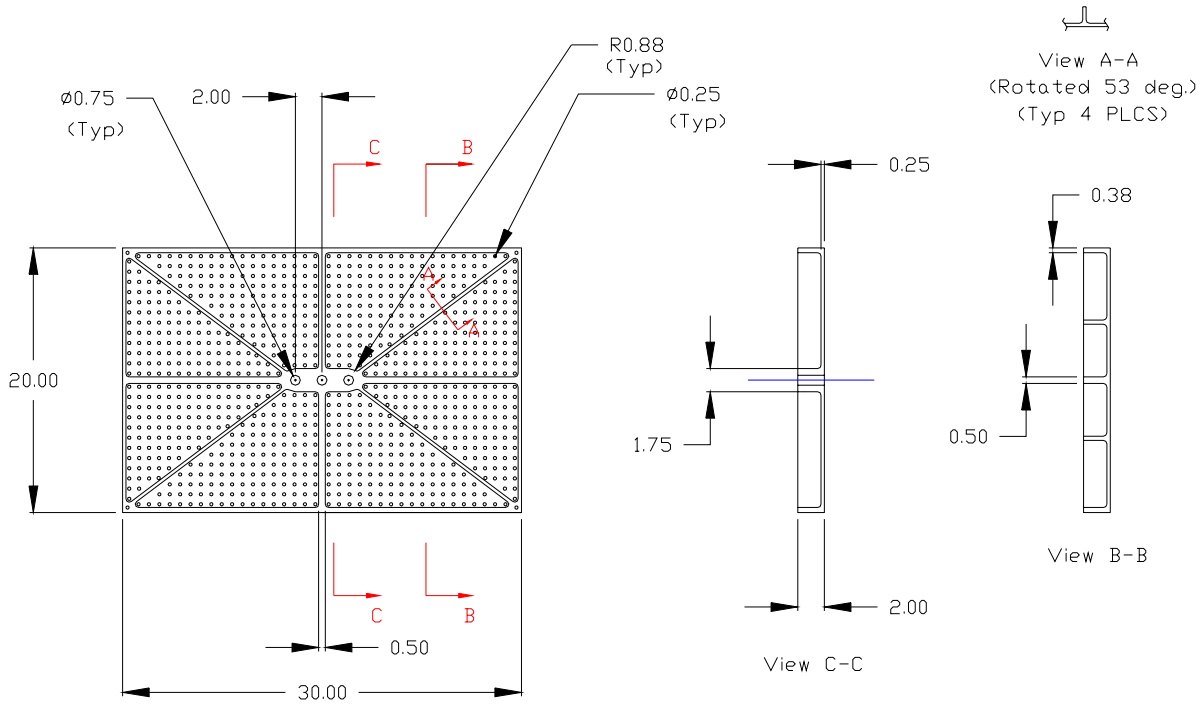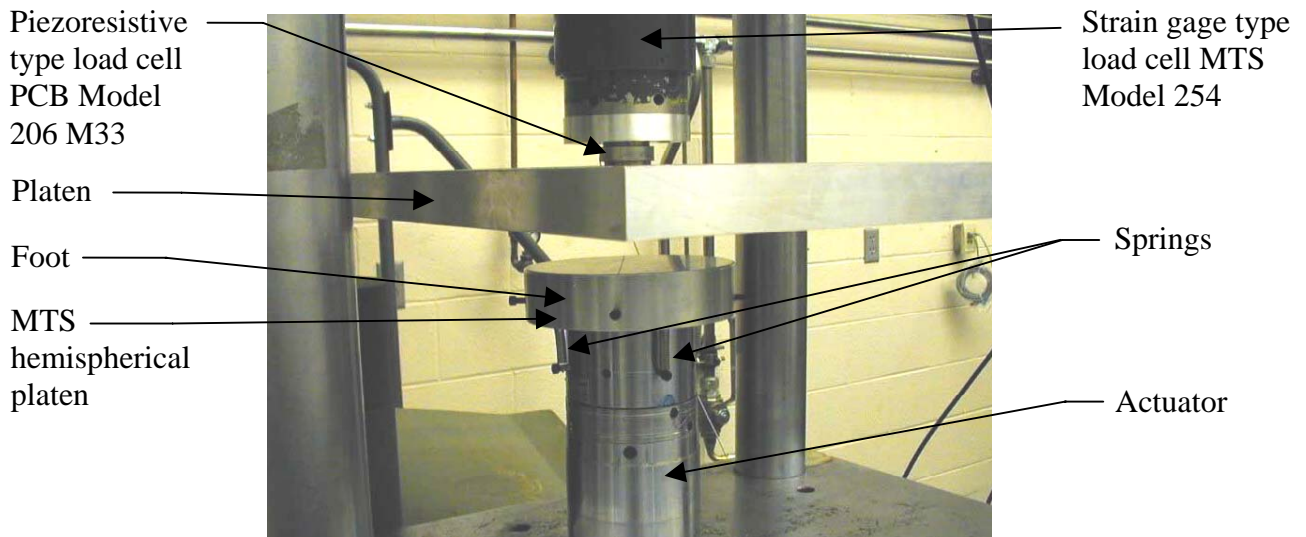

FIGURE 2-3. HIGH-RATE TEST SETUP

The apparatus was designed to accommodate 7 1/2-in.-diameter specimens, per ATSM D 3574-03, or full size bottom cushions, as shown in figure 2-4. The foot was designed as an 8-in.-diameter, self-aligning aluminum cap, which was placed over the MTS hemispherical platen. The springs that align the hemispherical platen are visible in this figure.

FIGURE 2-4. TYPICAL CUSHION TEST SETUPS

The upper platen was bolted to the load cell, which is bolted to the load frame's fixed cross beam. Cylindrical specimens are placed on the 8-in.-diameter foot prior to a test. Seat cushions were attached to the lower platen surface with Velcro hook and loop fasteners just as they are in typical seat installations. The "upside down" arrangement is advantageous since it enables the test to be performed by accelerating the lightest, smallest, and, therefore, stiffest items while restraining the heavier more flexible items in a fixed position. This arrangement tends to reduce the noise level in the data caused by the fixture response.

The load frame was controlled using the MTS Testar-IIm system. The MTS multipurpose testware (MPT) software was used to program the parameters for controlling the tests and acquiring data. This software was installed on the PC shown in figure 2-5. A procedure written in MPT specified the different test parameters, including displacement rates, data acquisition intervals, number of data points to acquire, etc. The high-rate procedure was subdivided into two main segments: a ramp up at 30 in./sec and a ramp down at 30 in./sec. Dynamic piezoresistive load cell data, static load cell data, and actuator displacement data were acquired simultaneously at 12,288 Hz. Simultaneous sample and hold data acquisition systems minimize the time skewing of acquired data by sampling all the data channels at the same time rather than sequentially at different times. Data from the piezoresistive load cell were acquired using the system described in the schematic shown in figure 2-6.

FIGURE 2-5. CONTROLLER
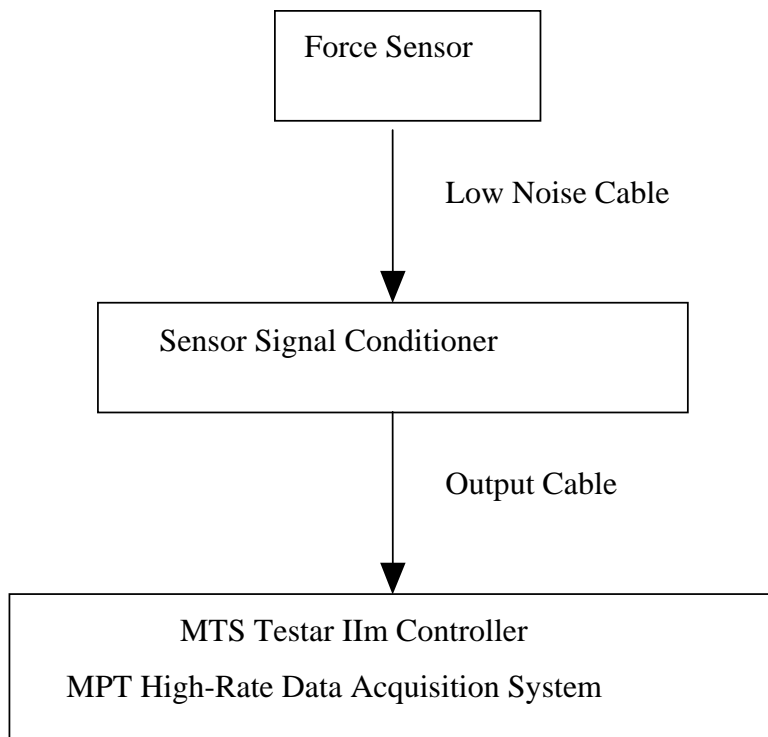
FIGURE 2-6. PIEZORESISTIVE LOAD CELL TEST SETUP

Typical actuator displacement and velocity time histories are shown in figures 2-7 and 2-8.
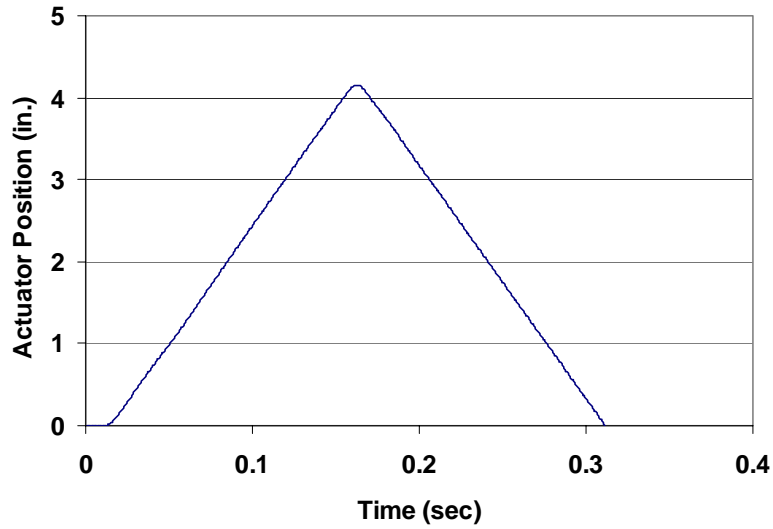
FIGURE 2-7. TYPICAL ACTUATOR POSITION VS TIME
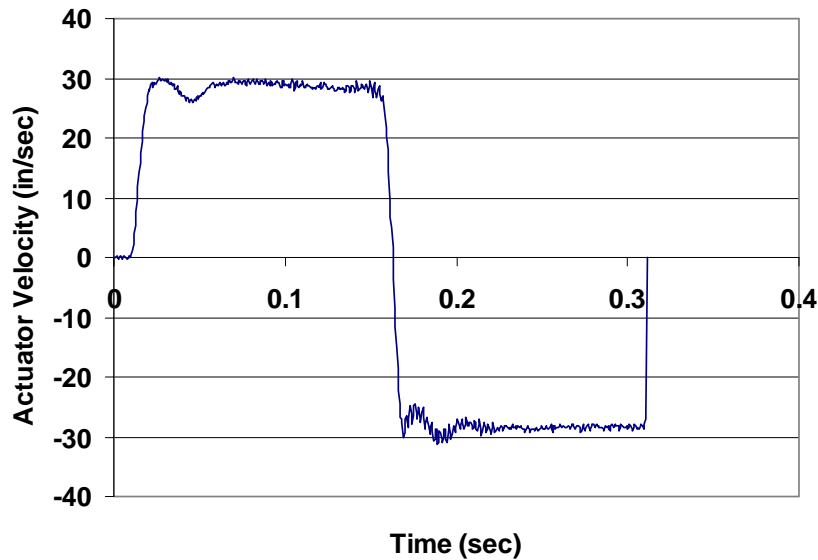
FIGURE 2-8. TYPICAL ACTUATOR VELOCITY VS TIME

Unfiltered displacement data are presented in figure 2-7. The velocity was computed using these unfiltered data and the standard central difference formula.

The static seat cushion test setup is shown in figures 2-9 and 2-10 and is similar to that used for the dynamic tests. These tests were conducted using a 22-kip load frame. The piezoresistive load cell was not used during these tests.
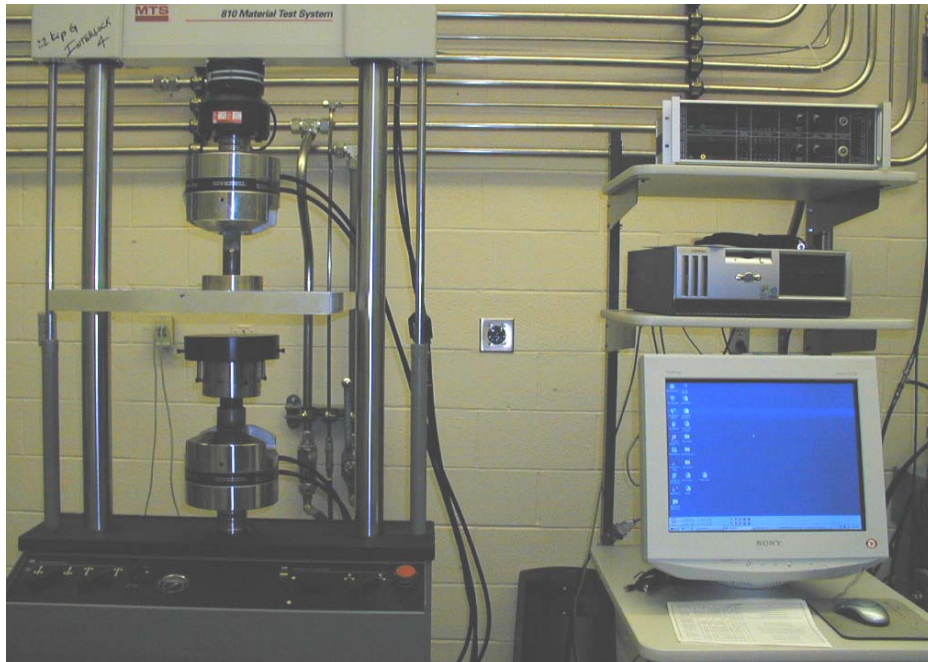
FIGURE 2-9. MTS 22-kip STATIC TEST SETUP

FIGURE 2-10. TYPICAL CUSHION STATIC TEST SETUP

The procedure used to conduct the static tests was very similar to the one used for dynamic tests with two segments: a ramp up at 0.033 in./sec and a ramp down at 0.033 in./sec. Static data, load and actuator displacement, were acquired at 151 Hz.

Piezoresistive load cells are typically used for dynamic testing and are commonly used for dynamic sled testing of aircraft seats. This type of load cell is constructed using a crystal material, as shown in figure 2-11(a). By comparison, standard strain gage-type load cells, typically used for static testing, are constructed using strain gages, as shown in figure 2-11(b). Conductivity in the piezoresistive load cell is influenced by a change (compression or stretching of the crystal grid) that is produced by a small deformation. The resistance change in a piezoresistive load cell is substantially higher than that in a standard strain gage-type load cell whose change in resistance is proportional to its strain. The supported mass in a piezoresistive load cell is much less than the supported mass in the standard strain gage-type load cell. Therefore, the former will produce less error due to inertia loading than the latter. Both the piezoresistive and the strain gage-type load cells were acquired in the dynamic material testing.

(a)   (b)
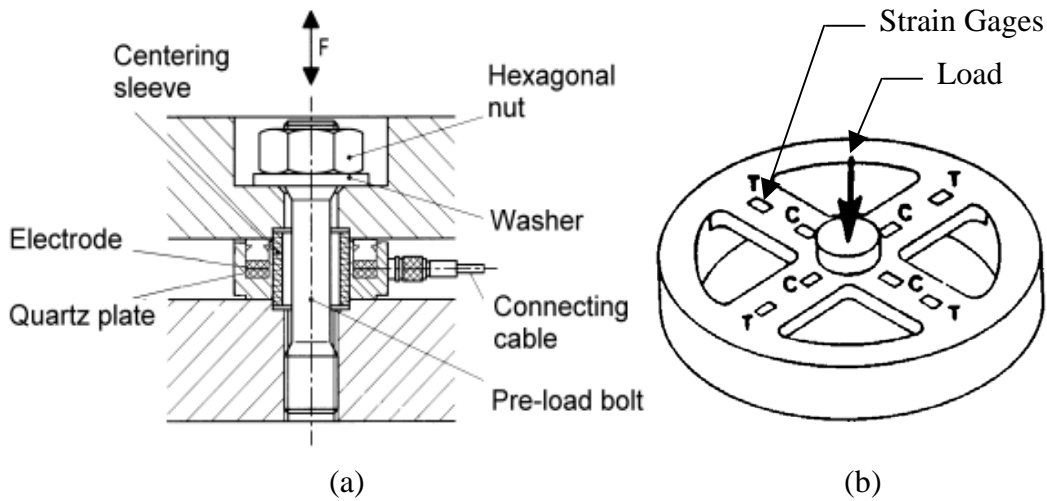
FIGURE 2-11. PIEZORESISTIVE AND STRAIN GAGE LOAD CELL

2.2 TEST ARTICLE DESCRIPTIONS.

Component material tests (static and dynamic) were conducted for the cushions. Dynamic rigid seat tests were performed for a subset of the cushion designs. The rectangular cushion geometry is defined in figure 2-12.

FIGURE 2-12. BOTTOM CUSHION GEOMETRY

The rectangular cushion specimens were fabricated with nominal dimensions of $d = 18.5$ in., $w = 19.0$ in., and thickness, t in., where the thickness, t, is defined in tables 2-1 and 2-2.
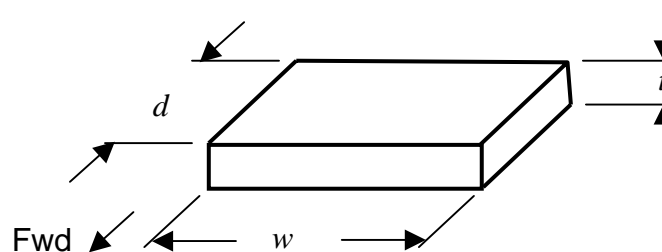
TABLE 2-1. NONFLOTATION BOTTOM CUSHIONS

Polymer A		Polymer B		Polymer C		Polymer D	
Density (lb/ft^3)	Thickness (in.)	Density (lb/ft^3)	Thickness (in.)	Density (lb/ft^3)	Thickness (in.)	Density (lb/ft^3)	Thickness (in.)
w_{A1}	2.0	w_{B1}	2.0	NA	NA	w_{D1}	2.0
w_{A1}	3.25	w_{B1}	3.25	NA	NA	w_{D1}	3.25
w_{A1}	4.5	w_{B1}	4.5	NA	NA	w_{D1}	4.5
w_{A2}	2.0	w_{B2}	2.0	w_{B2}	2.0	w_{D2}	2.0
w_{A2}	3.25	w_{B2}	3.25	w_{B2}	3.25	w_{D2}	3.25
w_{A2}	4.5	w_{B2}	4.5	w_{B2}	4.5	w_{D2}	4.5
w_{A3}	2.0	NA	NA	NA	NA	w_{D3}	2.0
w_{A3}	3.25	NA	NA	NA	NA	w_{D3}	3.25
w_{A3}	4.5	NA	NA	NA	NA	w_{D3}	4.5

Thickness tolerance = ±1/8 in.
Polymers B and C are expected to produce different IFDs, but will possess the same densities. (They are fabricated from the same polymer family.)

TABLE 2-2. LAMINATED (FLOTATION) BOTTOM CUSHIONS

Polymer A + Flotation 1		Polymer A + Flotation 2		Polymer B + Ethafoam	
Density (lb/ft^3)	Thickness (in.)	Density (lb/ft^3)	Thickness (in.)	Density (lb/ft^3)	Thickness (in.)
w_{A1}	$t_f + 1.0$	NA	NA	w_{B1}	$t_f + 1.0$
w_{A1}	$t_f + 3.0$	NA	NA	w_{B1}	$t_f + 3.0$
w_{A2}	$t_f + 1.0$	w_{A2}	$t_f + 1.0$	w_{B2}	$t_f + 1.0$
w_{A2}	$t_f + 3.0$	w_{A2}	$t_f + 3.0$	w_{B2}	$t_f + 3.0$
w_{A3}	$t_f + 1.0$	NA	NA	NA	NA
w_{A3}	$t_f + 3.0$	NA	NA	NA	NA

Thickness tolerance = ±1/8 in.
The densities herein refer to the density of the nonflotation comfort foam.
t_f = the thickness of the flotation foam (nominally $t_f = 1.0$ in.) and is a constant for a given polymer.

The cylindrical cushion specimens are 7 1/2 in. in diameter, as specified in ASTM D 3574-03. The upper and lower surfaces of the specimens were required to be parallel. Figures 2-13 and 2-14 show the numbering scheme used to identify the specimens.

NαwαiCT_xxx

— serial number

— thickness

— Specimen type (C denotes cylinder, R denotes rectangular)

— Specimen density (for comfort foam α, density i)
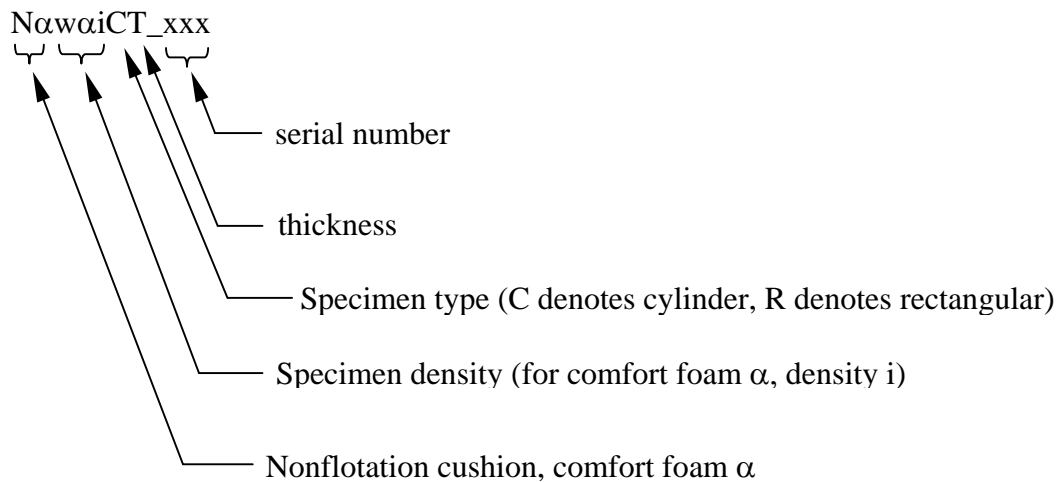
— Nonflotation cushion, comfort foam α

FIGURE 2-13. NONFLOTATION CYLINDRICAL SPECIMEN NUMBERING SCHEME

For example, the number NAwa3R200_510 denotes a rectangular nonflotation cushion, comfort foam A (or a), density w_{A3}, thickness code 200, and serial number 510.

FαβwαiCT_xxx

— serial number

— thickness

— Specimen type (C denotes cylinder, R denotes rectangular)

— Specimen density (for comfort foam α, density i)

— Flotation cushion, comfort foam α. flotation foam β
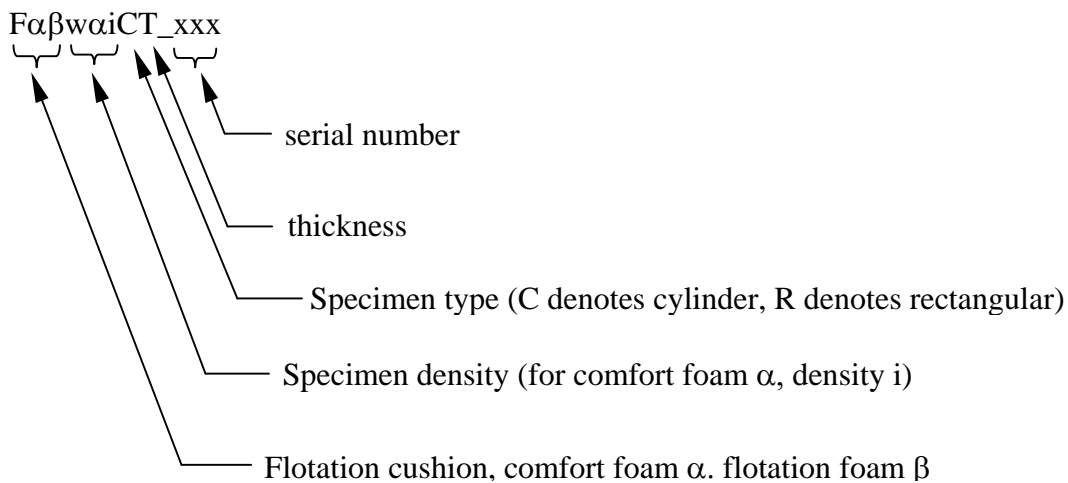
FIGURE 2-14. LAMINATED FLOTATION CYLINDRICAL SPECIMEN
NUMBERING SCHEME

For example, the number FAF2wa2C325_600 denotes a cylindrical laminated (flotation) cushion, comfort foam A (or a), density w_{A2}, thickness code 325, and serial number 600. The test program used the specimens identified in tables 2-1 and 2-2. The test articles were fabricated from comfort foam materials with densities ranging from 3.1 to 4.3 lb/ft^3.

The flotation specimens consisted of a layer of nonflotation comfort foam that was bonded on top of a nominal 1-in. layer of flotation foam. The specific thickness of the flotation foam was established to satisfy the flotation requirements of TSO-C72c and, thus, varied for each flotation foam material.

The densities of the nonflotation comfort foams and flotation foams are summarized in table 2-3. The flotation cushions, being laminated, were constructed with a layer of comfort foam bonded on top of a layer of flotation foam. The nonflotation cushions, thus, had the same densities as the nonflotation foams. However, the flotation cushions contained densities somewhat greater than the densities of the flotation foam. The same comfort foam materials were used in the fabrication of the flotation and nonflotation cushions.

TABLE 2-3. FOAM DENSITIES

Nonflotation		Flotation	
Material	w (lb/ft^3)	Material	w (lb/ft^3)
NAwa1	4.3	Flotation 1	1.5
NAwa2	3.8	Flotation 2	2.2
NAwa3	4.3	Flotation 3	1.7
NBwb2	4.3	ETHAfoam	2.4
NCwb2	3.4		
NDwd1	3.1		
NDwd2	3.2		
NDwd3	4.4		

A muslin cover was bonded to the upper and lower surfaces of test articles fabricated from fire-hardened materials such as DAX foam. A fire-blocking material was bonded to the bottom surface and a muslin cover to the upper surface of test articles fabricated from other materials.

2.3 TEST PROCEDURE.

The data recording procedure consisted of defining a specimen name and entering it into the MPT program. A digital still photograph was taken of the test setup, then the test was conducted.

The tests were conducted in stroke control, i.e., loads were imposed as specified displacements. Stroke control was selected rather than load control since this is less likely to damage the fixtures and transducers. The system is capable of generating loading rates up to 30 in./sec for the amount of stroke required during these tests.

An examination of the test results reveals some oscillations in the unloading curve. These continue to the end of the test and may be the modal response of the upper platen to the impulsive loading, or they might reflect the intrinsic dynamic response of the servohydraulic system. In any event, they do not pose a problem in terms of extracting the material properties from the data.

3. RESULTS.

3.1 MATERIAL TEST RESULTS.

The unfiltered material test data acquired during testing of the cylindrical specimens are presented in figures 3-1 through 3-5 for the nonflotation and laminated (flotation) cushions, respectively.
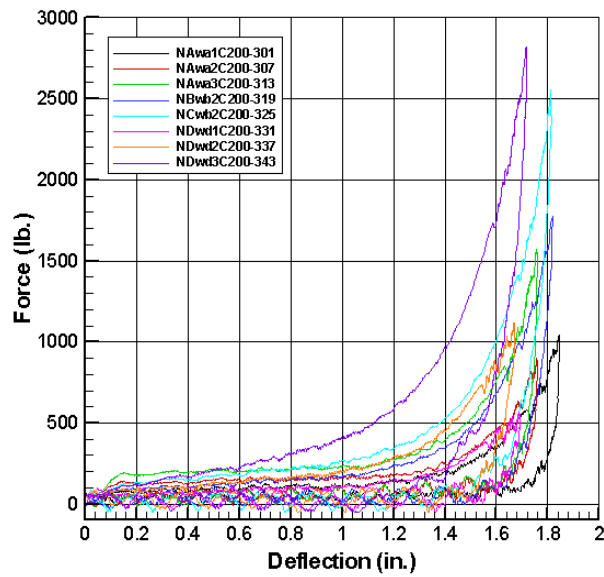

FIGURE 3-1. LOAD-DEFLECTION CURVE FOR 2-in. NONFLOTATION CUSHION SPECIMENS
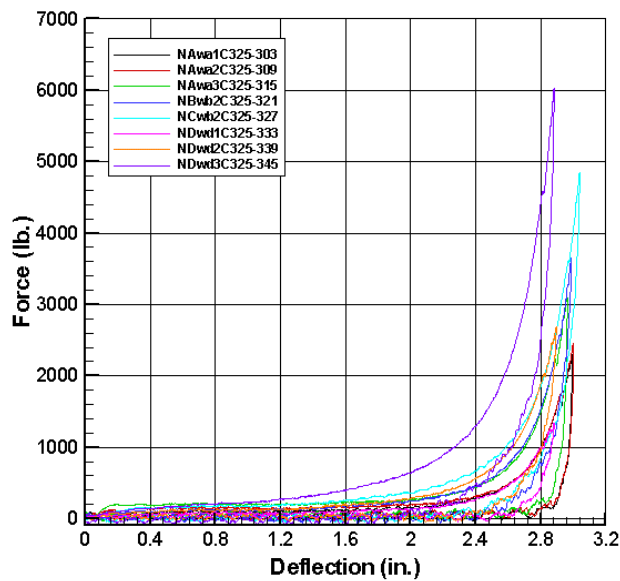

FIGURE 3-2. LOAD-DEFLECTION CURVE FOR 3 1/4-in. NONFLOTATION CUSHION SPECIMENS
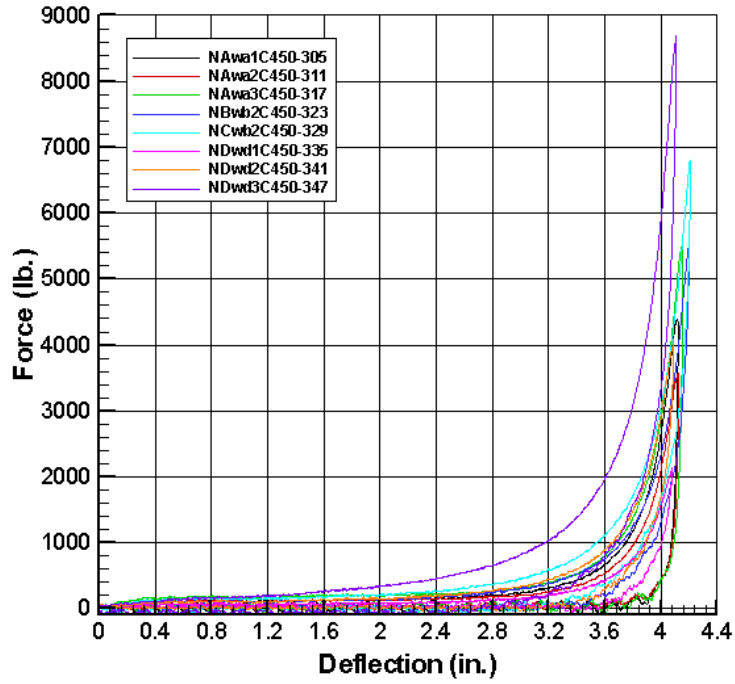
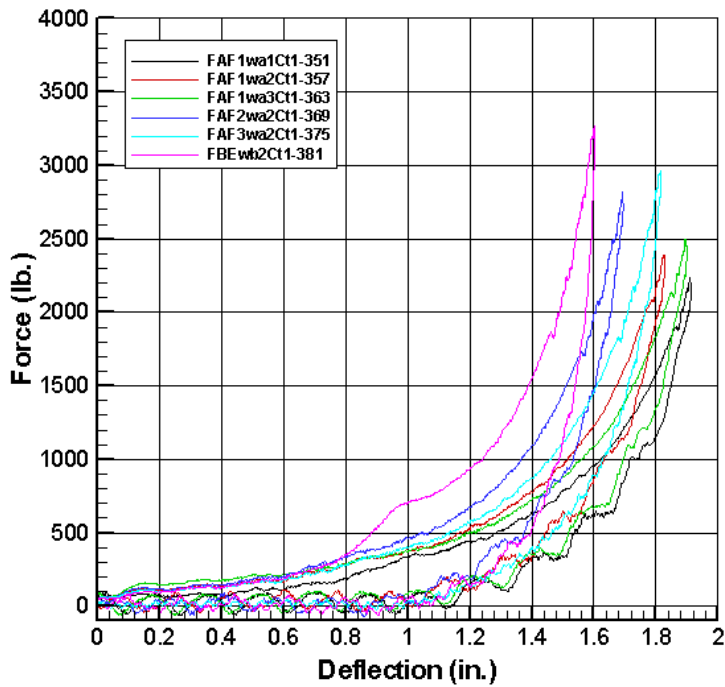FIGURE 3-3. LOAD-DEFLECTION CURVE FOR 4 1/2-in. NONFLOTATION
CUSHION SPECIMENS

FIGURE 3-4. LOAD-DEFLECTION CURVE FOR 2-in. FLOTATION
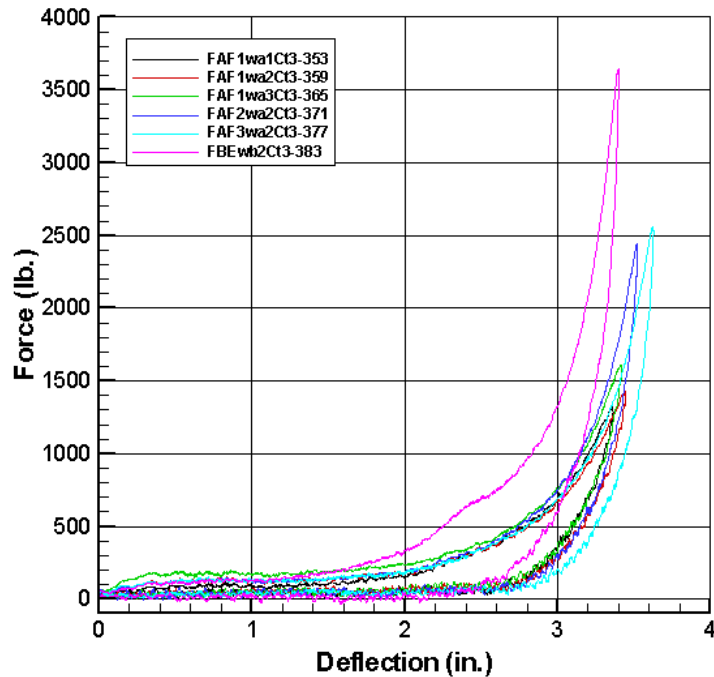CUSHION SPECIMENS

FIGURE 3-5. LOAD-DEFLECTION CURVE FOR 4-in. FLOTATION
CUSHION SPECIMENS

The third set of flotation cushions were defined as the required thickness of flotation foam without the usual layer of comfort foam.

A number of cushion tests were conducted at the FAA CAMI to the conditions specified in 14 CFR 25.562(b)(1), as described in section 1.2. The cushion test articles corresponded to specific material test articles, which were fabricated with the same lamination design. The sled test articles were selected to obtain lumbar load data for the strongest, weakest, and intermediate strength materials. At least three cushions were tested for each cushions thickness. In selected cases, five cushions were tested. The CAMI sled test results are summarized in tables 3-1 and 3-2. These results have all been scaled to a 14-g deceleration impulse. The cushion-loading rate produced during these sled tests was established from photometric analyses of the data and found to range from 42-108 in./sec [22].

TABLE 3-1. SUMMARY OF SLED TEST RESULTS FOR NONFLOTATION CUSHIONS

Material	NAwa3	Nawa2	NCwb2	NDwd1	NDwd3
Thickness (in.)	Lumbar Load (lb)				
2	1856.2			1173.1	1232.5
2				1186.5*	
3 1/4	1778.7			1199.7	1195.0
3 1/4					1171.9
4 1/2	1698.5	2136.7	1794.5	1253.8	1155.8

* Repeat test

TABLE 3-2. SUMMARY OF SLED TEST RESULTS FOR FLOTATION CUSHIONS

Material	FAF1wa1	FAF1wa2	FAF1wa3	FAF2wa2	FAF3wa2	FBEwb2
Thickness (in.)	Lumbar Load (lb)					
1		1127.3		1178.6		1085.1
2	1300.7	1465.6	1408.1	1313.9		1261.4
4		1829.7	1761.4	1839.7	1834.9	1410.7

3.2 NONFLOTATION MONOLITHIC CUSHIONS RESULTS.

The load-deflection curves acquired during dynamic component tests of the nonflotation cushions are presented in figures 3-6 through 3-8. The scaled lumbar loads acquired during the CAMI sled tests are presented as well. The term scaled lumbar load refers to the lumbar load that is computed to a 14-g impulse.

A few general observations are in order before analyzing the properties of this material in detail. When comparing these curves, the most distinguishing feature is the plateau strength. It is important to remember that the peak strength on the right-hand side of these plots is an artifact of the particular test, since this magnitude is not a material property but simply depends on the maximum displacement of the actuator. The maximum possible magnitude of the peak load is limited either by the capability of the test stand or the melting pressure of the foam's cell wall material.

Load-deflection curves for three different thicknesses of this material are presented in figure 3-9, and the scaled lumbar load is plotted versus thickness in figure 3-10.
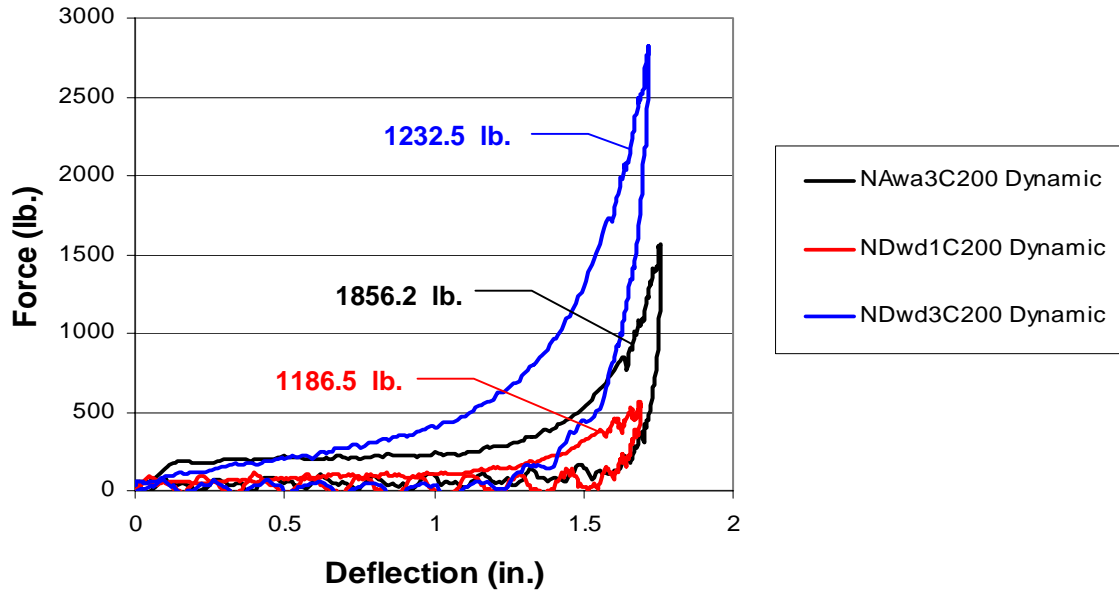
FIGURE 3-6. LOAD-DEFLECTION CURVE FOR 2-in. NONFLOTATION (COMFORT)
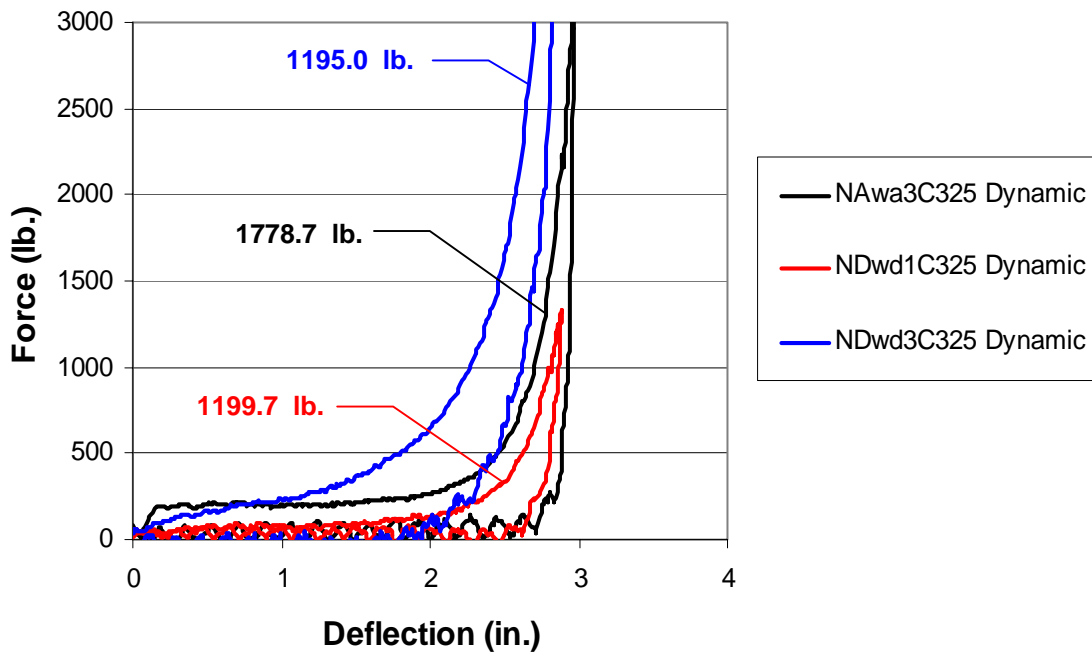FOAM SPECIMENS

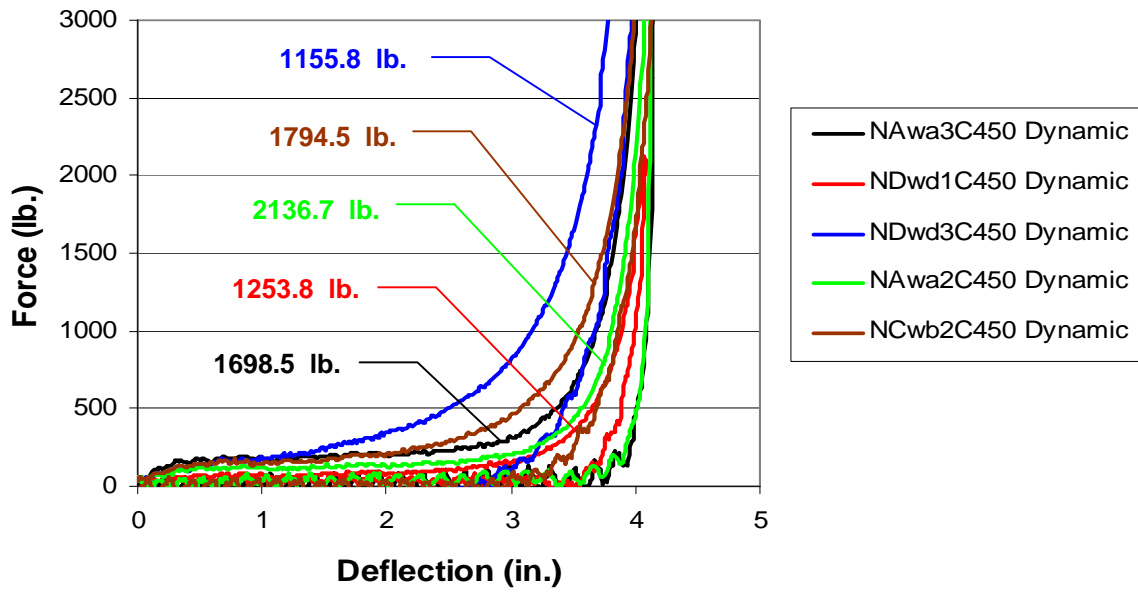FIGURE 3-7. LOAD-DEFLECTION CURVE FOR 3 1/4-in. NONFLOTATION (COMFORT)
FOAM SPECIMENS

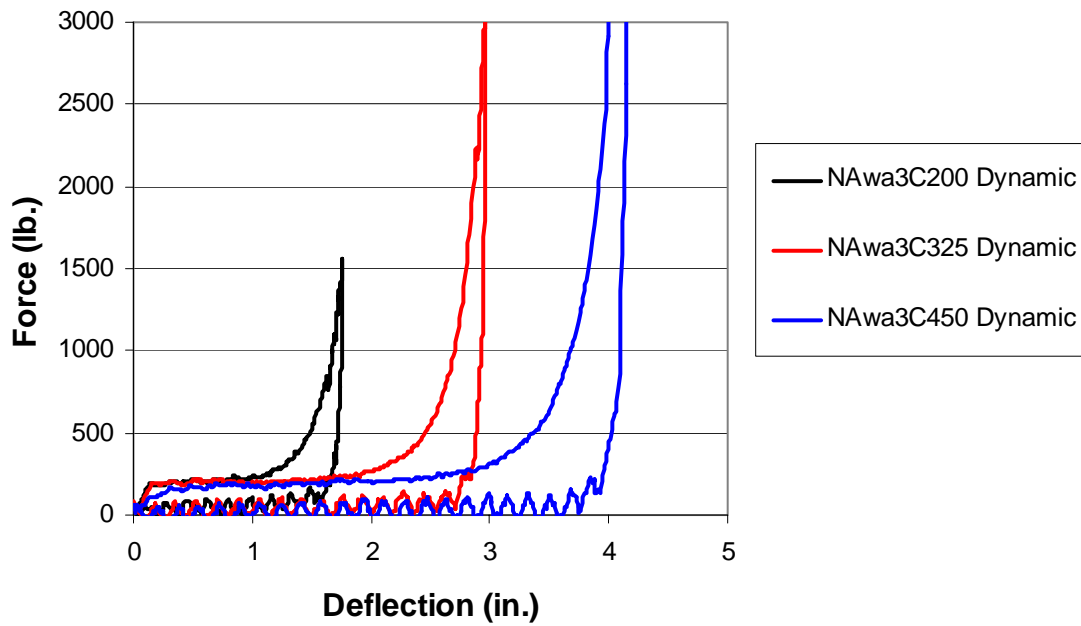FIGURE 3-8. LOAD-DEFLECTION CURVE FOR 4 1/2-in. NONFLOTATION (COMFORT) FOAM SPECIMENS

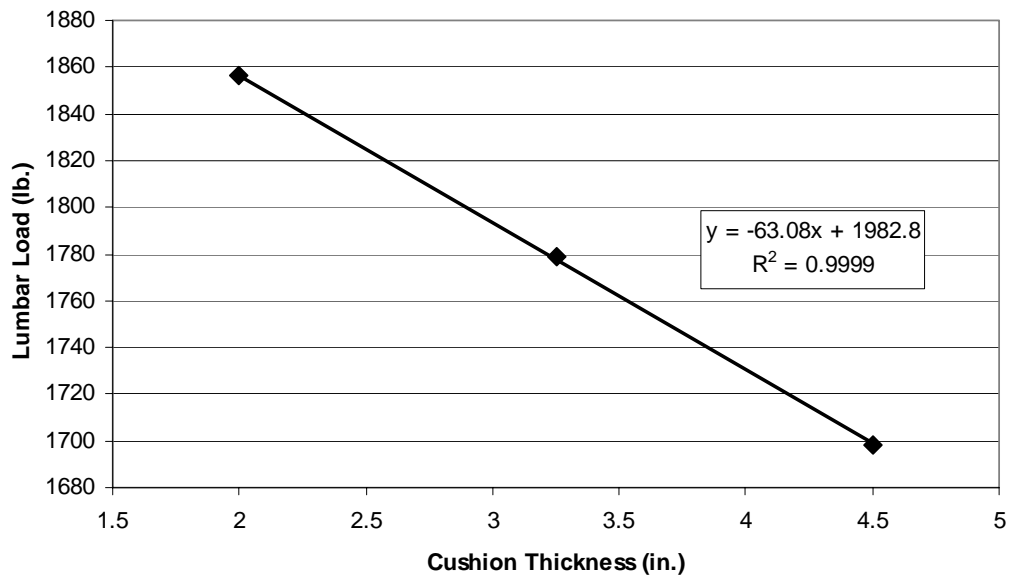FIGURE 3-9. NAwa3 LOAD-DEFLECTION CURVES FOR VARIOUS SPECIMEN THICKNESSES

FIGURE 3-10. LUMBAR LOAD VS CUSHION THICKNESS FOR NAwa3 SPECIMENS

The fact that the load-deflection data generate generic material properties is established by computing stress-strain curves from these data. The stress-strain curves, which correspond to the load-deflection curves presented in figure 3-9, are presented in figure 3-11.

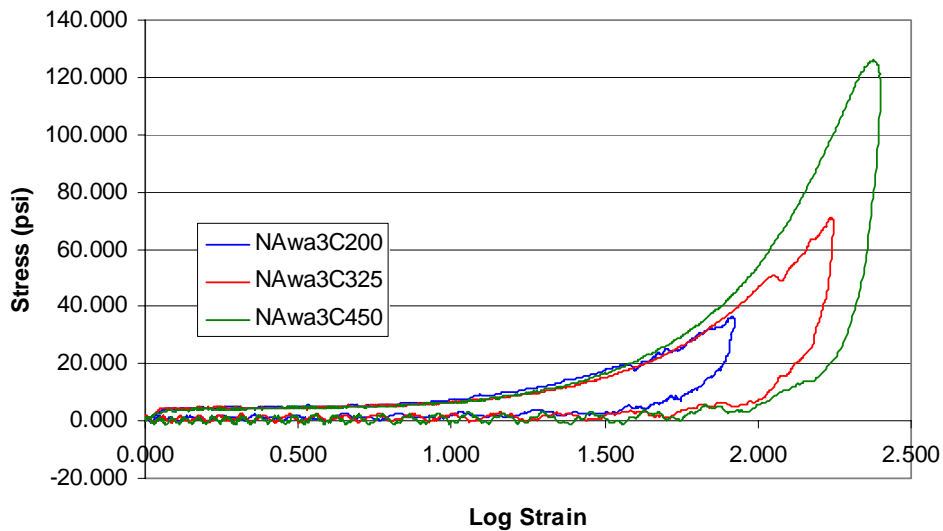FIGURE 3-11. STRESS-STRAIN CURVES FOR NAwa3 SPECIMENS

To evaluate whether these are generic data, the unloading curves for the 3 1/4- and 4 1/2-in. specimens, i.e., curves NAwa3C325 and NAwa3C450, are shifted to the left so that they intersect their loading curves at a log strain of 1.917. This is the standard procedure for a material nonlinear analysis and results in the stress-strain curves presented in figure 3-12.
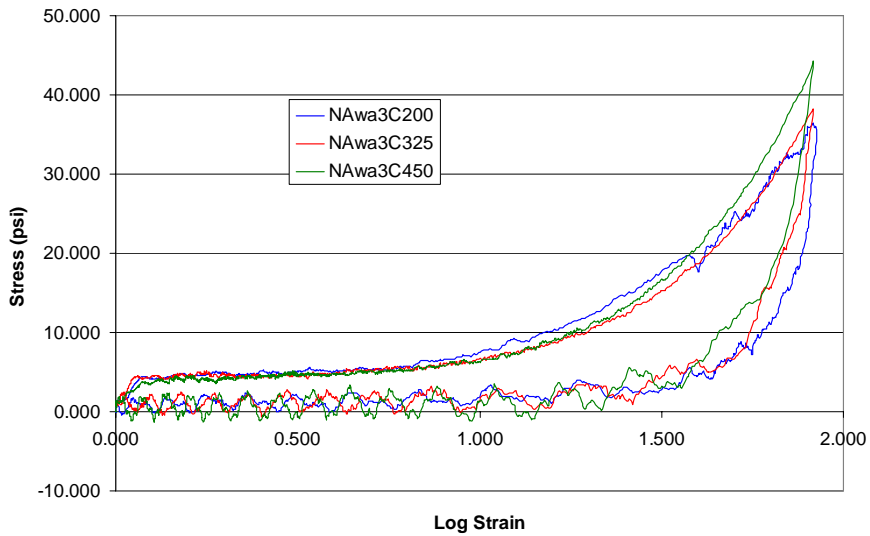
FIGURE 3-12. EQUIVALENCE OF NAwa3 STRESS-STRAIN CURVES

The significance of the unloading curves and their significance on lumbar load is not as obvious as the significance of the loading curve. The unloading characteristics undoubtedly affect lumbar load, but it is not possible to quantify this effect without knowing the magnitude of the cushion load during the seat test. This load level varies from test to test and cushion to cushion.

3.3 LAMINATED (FLOTATION) CUSHIONS RESULTS.

The load-deflection curves for the laminated cushions are shown in figure 3-13. The first set of laminated cushions was constructed as a 1-in. layer of soft comfort foam that was bonded on top of a layer of flotation foam. The thickness of the flotation foam was determined so that the cushion would satisfy the flotation requirements.
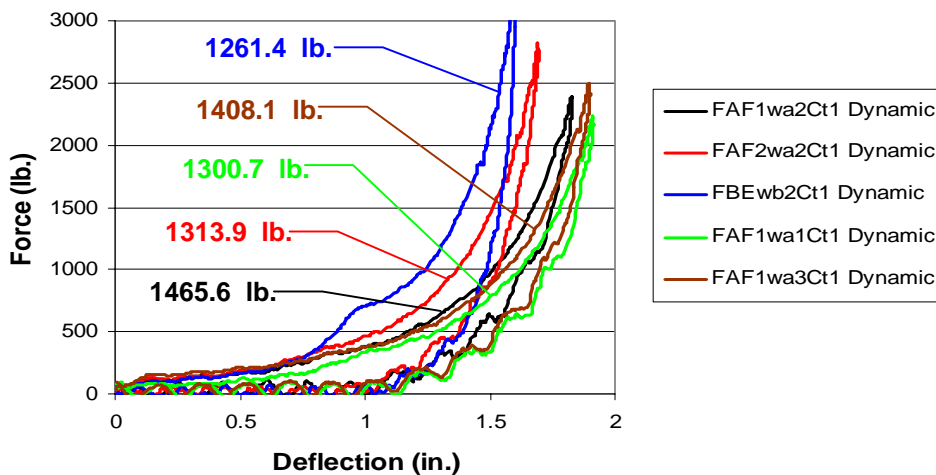

FIGURE 3-13. LOAD-DEFLECTION CURVES FOR Ct1 LAMINATED SPECIMENS

3-8

A second set of laminated cushions was constructed of a 3-in. layer of soft comfort foam that was bonded on top of a layer of flotation foam.

Examining figures 3-13 and 3-14, it is seen that these curves haves a form similar to that exhibited by the nonflotation cushions; however, the data does not bracket the curve developing the maximum lumbar load in figure 3-14 and barely brackets it in figure 3-13. One cannot reliably identify a relative maximum lumbar load in these figures.
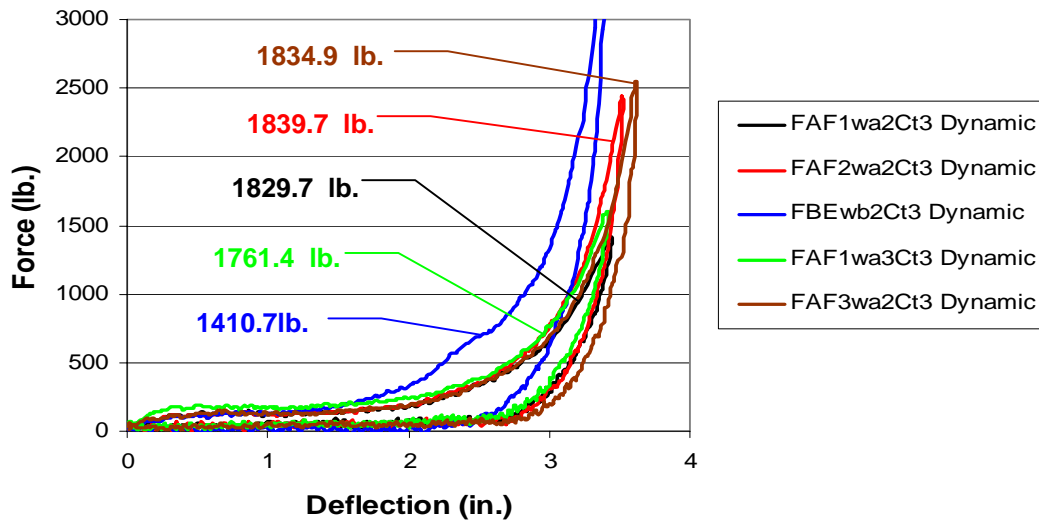
FIGURE 3-14. LOAD-DEFLECTION CURVES FOR Ct3 LAMINATED SPECIMENS

The stress-strain data presented in figure 3-12 was used to compute criteria curves for the 2-in. (Ct1) and 4-in. (Ct3) cushion thicknesses. The corresponding lumbar loads were computed for the criteria curves using the linear regression presented in figure 3-10. The results are presented in figures 3-15 and 3-16.
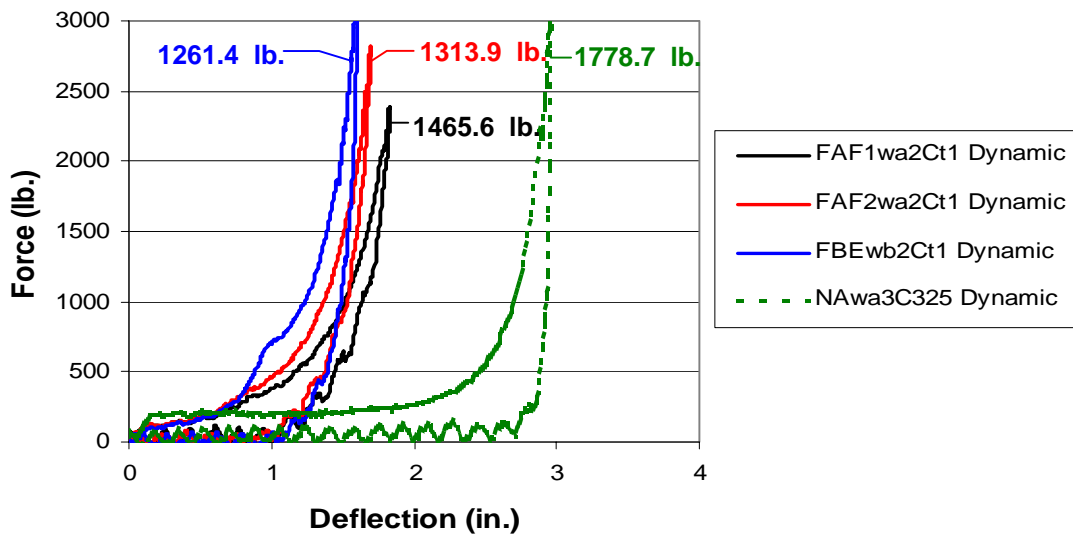

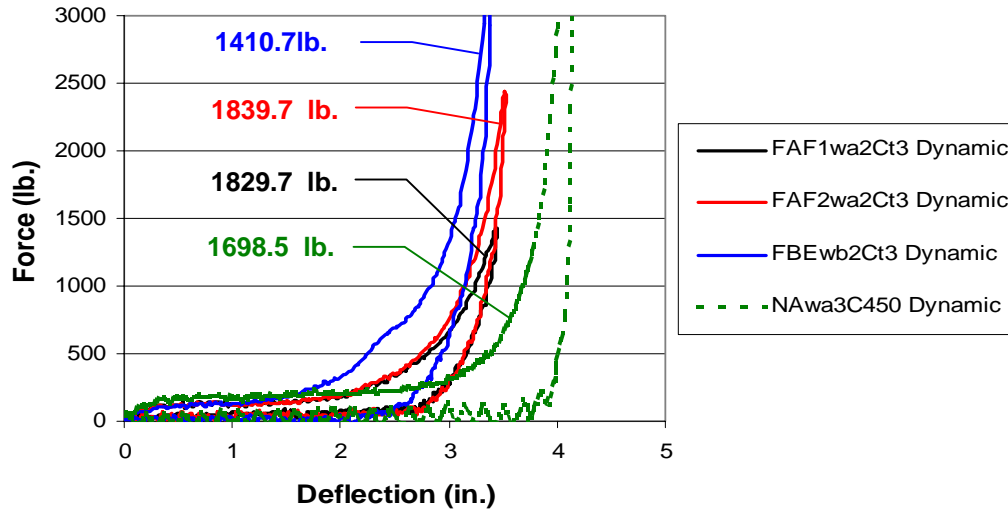FIGURE 3-15. LOAD-DEFLECTION CURVES FOR Ct1 LAMINATED SPECIMENS

FIGURE 3-16. LOAD-DEFLECTION CURVES FOR Ct3 LAMINATED SPECIMENS

These results show that the criterion curve proposed for the nonflotation cushions is inappropriate for use with the laminated flotation cushions. The reason is due to the significant difference in the densification displacements of the flotation cushions, which are much lower than the densification displacements of the nonflotation cushions. This represents a significant difference between the responses of flotation and nonflotation cushions.

3.4 STATIC TEST RESULTS.

A series of static tests were performed to address two issues: (1) to assess the rate sensitivity of these foam cushions and (2) to assess whether the component test could use static testing rather than dynamic testing. The static test data for the cylindrical test specimens are presented in figures 3-17 through 3-22.

FIGURE 3-17. LOAD-DEFLECTION CURVES FOR 2-in. NONFLOTATION
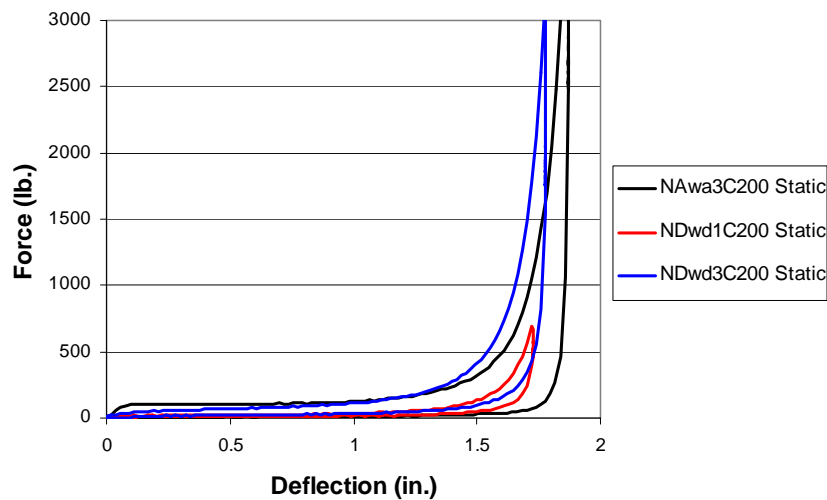(COMFORT) SPECIMENS

3-10
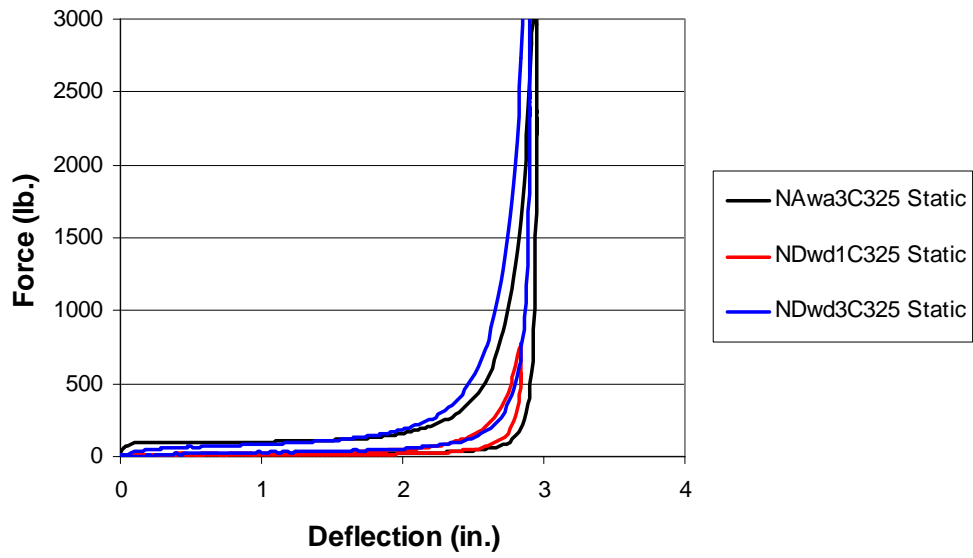
FIGURE 3-18. LOAD-DEFLECTION CURVES FOR 3 1/4-in. NONFLOTATION
(COMFORT) FOAM SPECIMENS
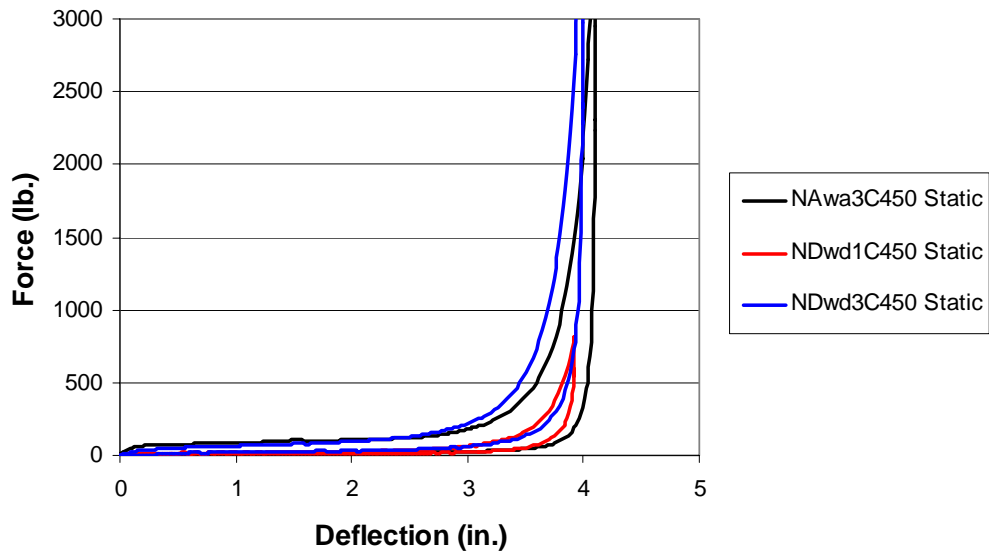
FIGURE 3-19. LOAD-DEFLECTION CURVES FOR 4 1/2-in. NONFLOTATION
(COMFORT) FOAM SPECIMENS

FIGURE 3-20. NAwa3 LOAD-DEFLECTION CURVES FOR VARIOUS NONFLOTATION
FOAM SPECIMEN THICKNESSES

FIGURE 3-21. NDwd1 LOAD-DEFLECTION CURVES FOR VARIOUS NONFLOTATION
FOAM SPECIMEN THICKNESSES
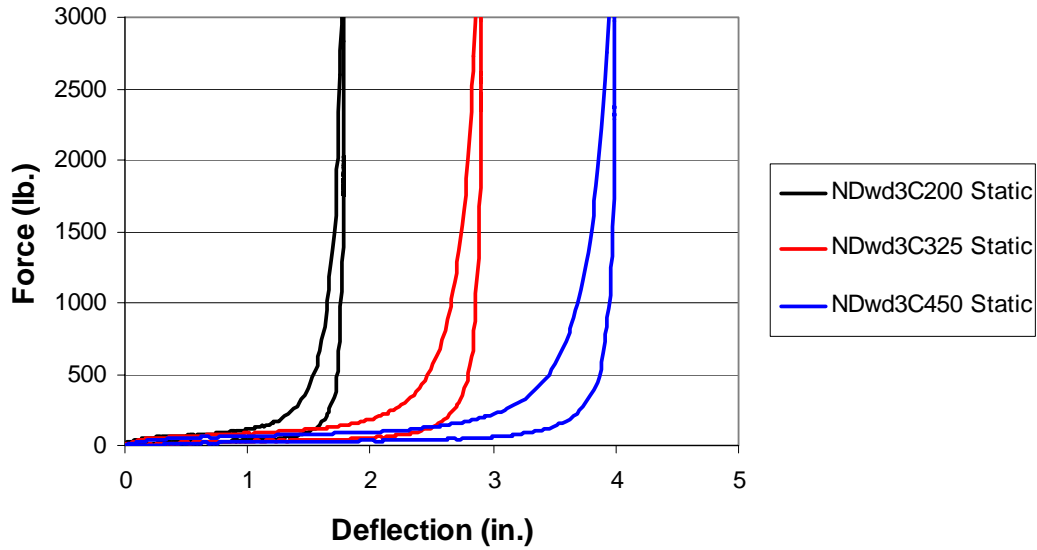
FIGURE 3-22. NDwd3 LOAD-DEFLECTION CURVES FOR VARIOUS NONFLOTATION
FOAM SPECIMEN THICKNESSES

The static test results of the flotation cushions are presented in figures 3-23 through 3-28. These
figures illustrate the effects of varying the thickness of the comfort foam layer. Recall that the
data presented in figure 3-23 are for specimens fabricated of flotation foam only.
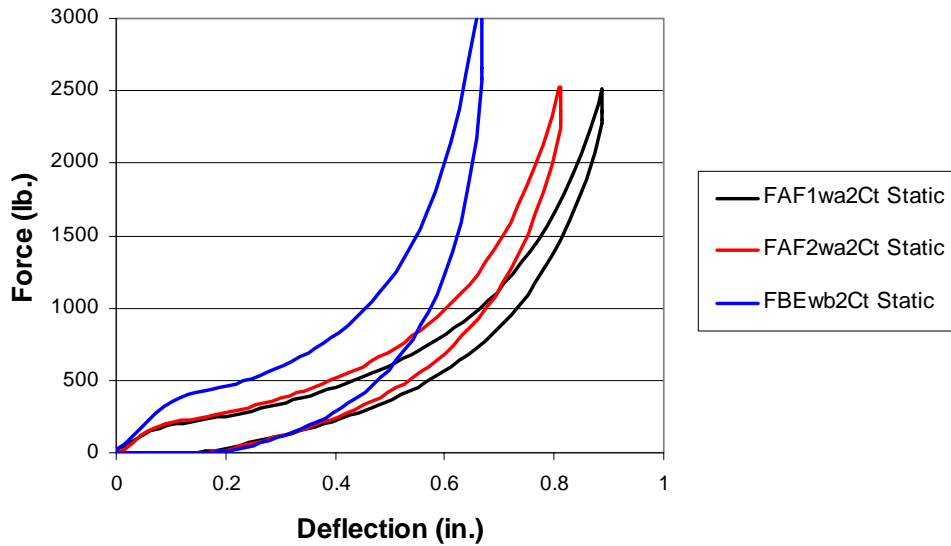
FIGURE 3-23. LOAD-DEFLECTION CURVES FOR Ct LAMINATED
FLOTATION SPECIMENS
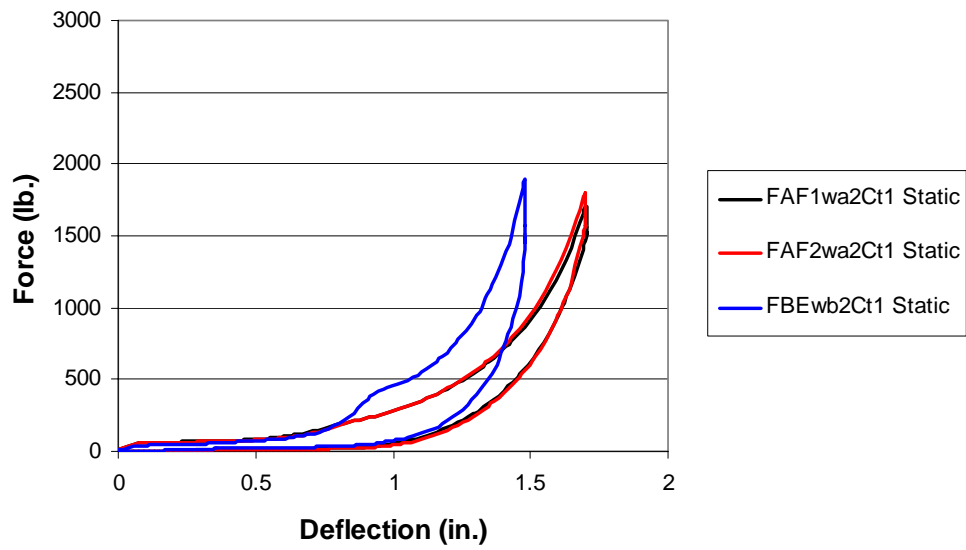
FIGURE 3-24. LOAD-DEFLECTION CURVES FOR Ct1 LAMINATED
FLOTATION SPECIMENS

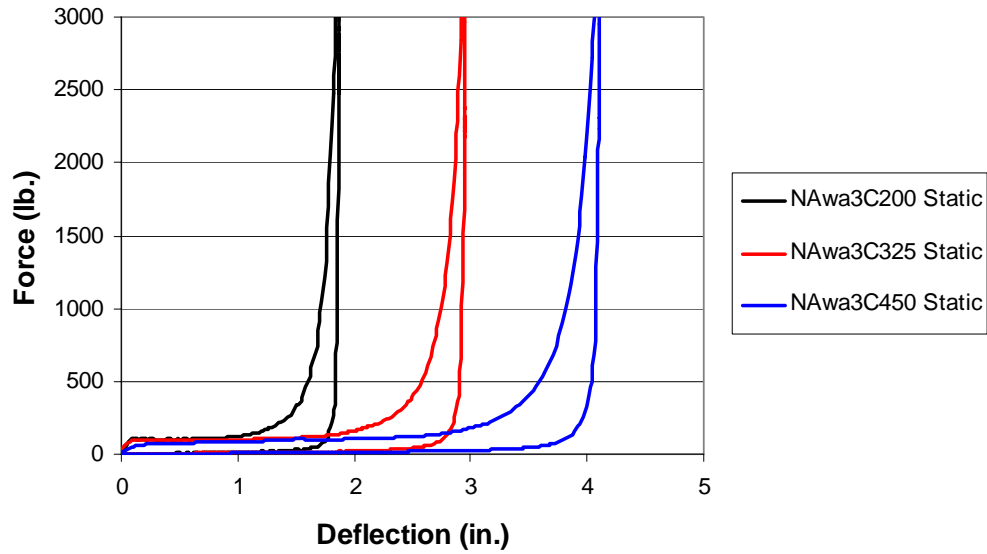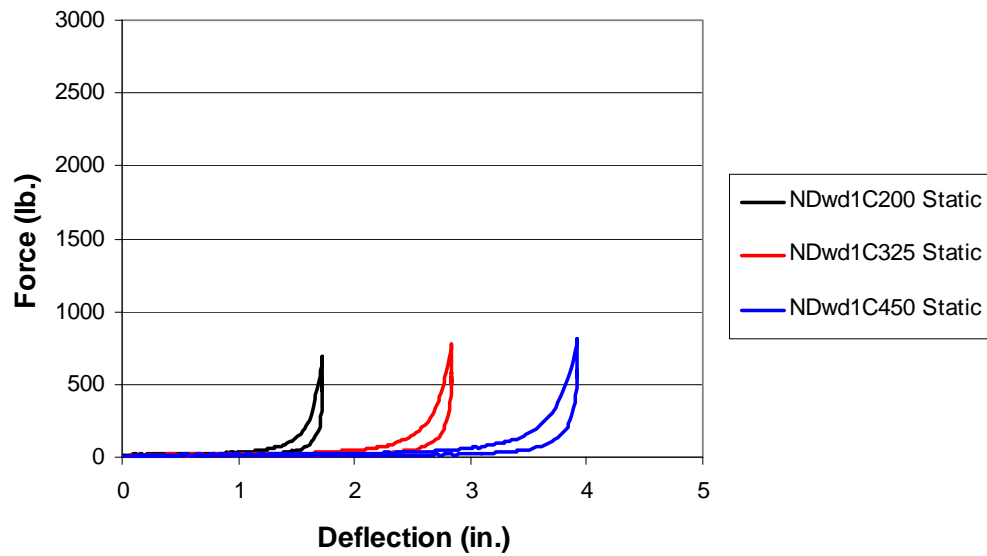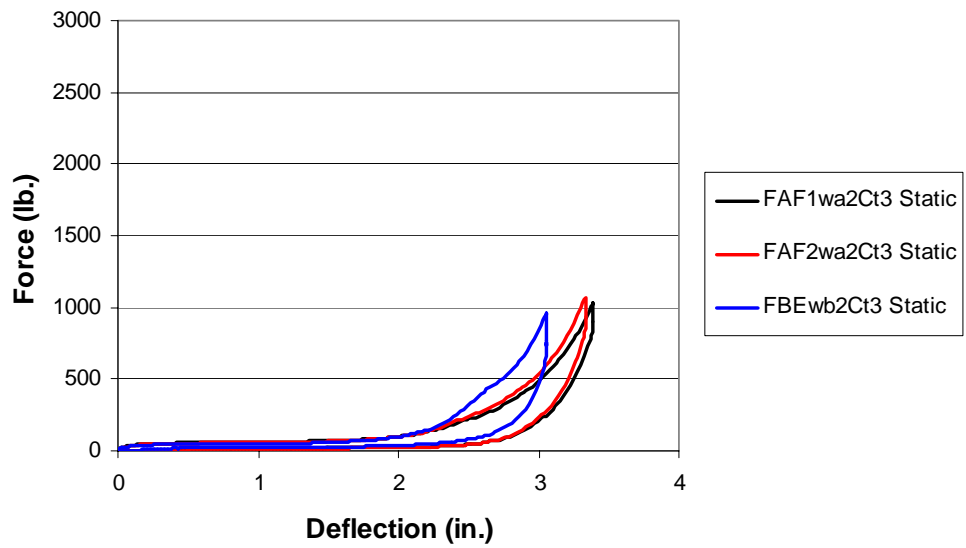FIGURE 3-25. LOAD-DEFLECTION CURVES FOR Ct3 LAMINATED
FLOTATION SPECIMENS
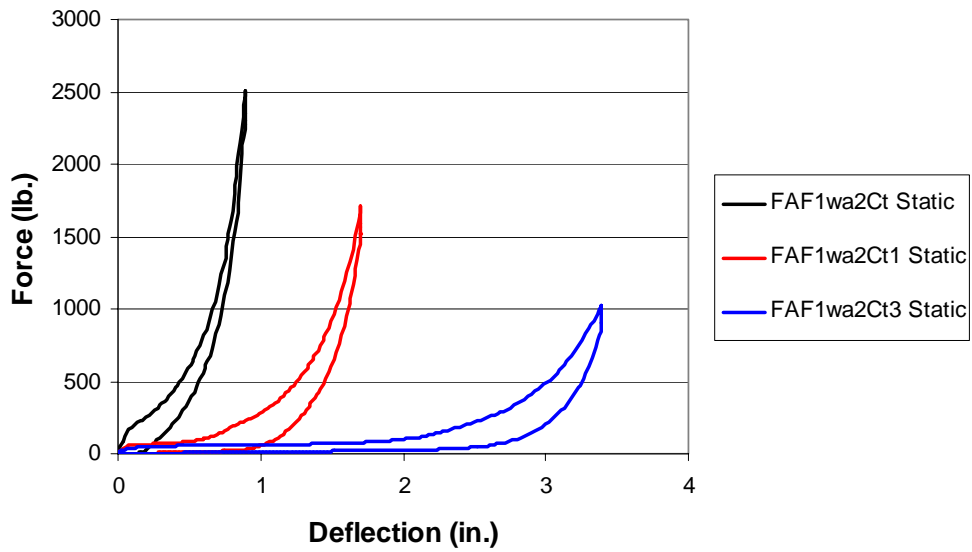
FIGURE 3-26. FAF1wa2 LOAD-DEFLECTION CURVES FOR VARIOUS FLOTATION
SPECIMEN THICKNESSES
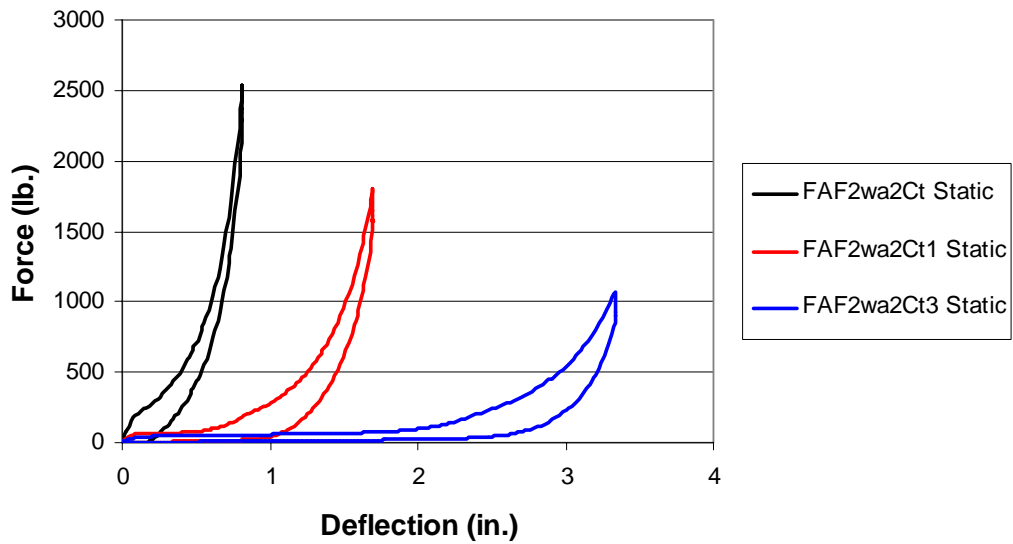
FIGURE 3-27. FAF2wa2 LOAD-DEFLECTION CURVES FOR VARIOUS FLOTATION
SPECIMEN THICKNESSES
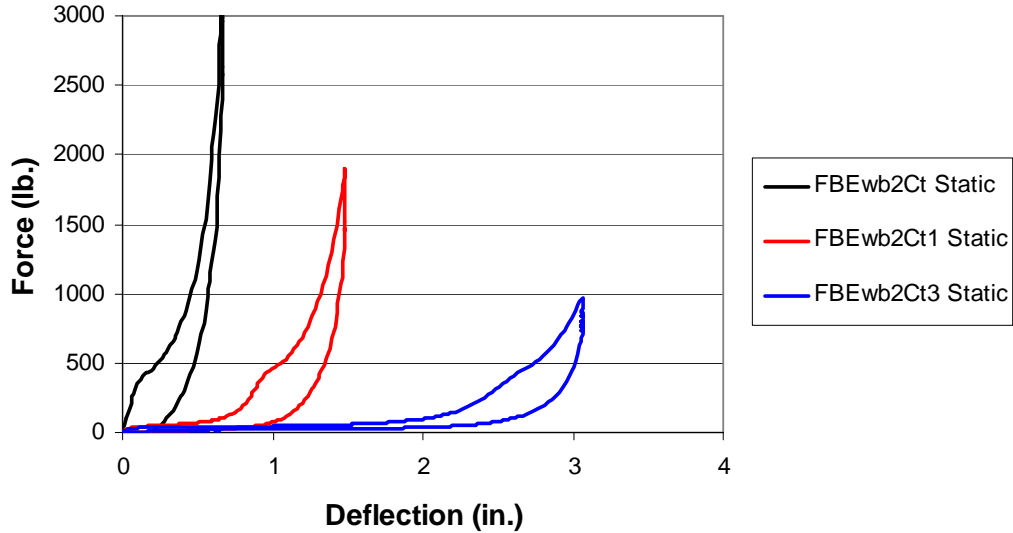
FIGURE 3-28. FBEwb2 LOAD-DEFLECTION CURVES FOR VARIOUS FLOTATION
SPECIMEN THICKNESSES

Static component tests were conducted using the modified ASTM D 3574 IFD procedure to determine whether they could be used rather than the dynamic test procedure. The results from these tests are presented in figures 3-29 through 3-31. Cylindrical specimens were used in both series of these tests. Results for the nonflotation specimens are presented first.
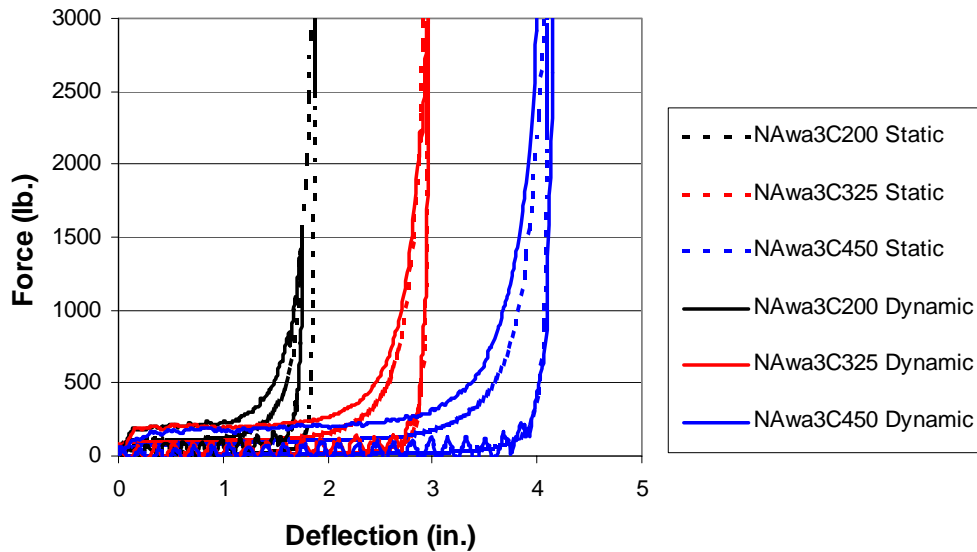
FIGURE 3-29. STATIC AND DYNAMIC TEST RESULTS FOR NAwa3
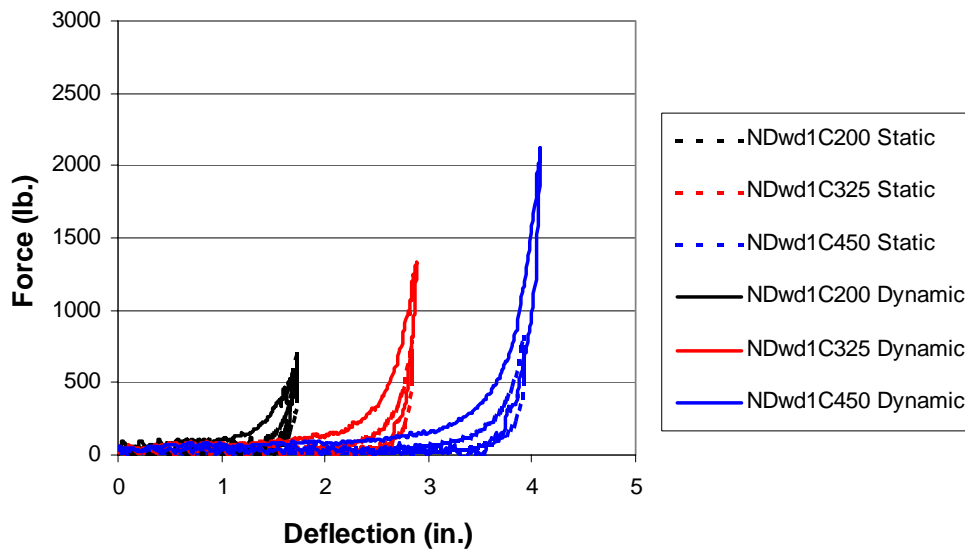
FIGURE 3-30. STATIC AND DYNAMIC TEST RESULTS FOR NDwd1
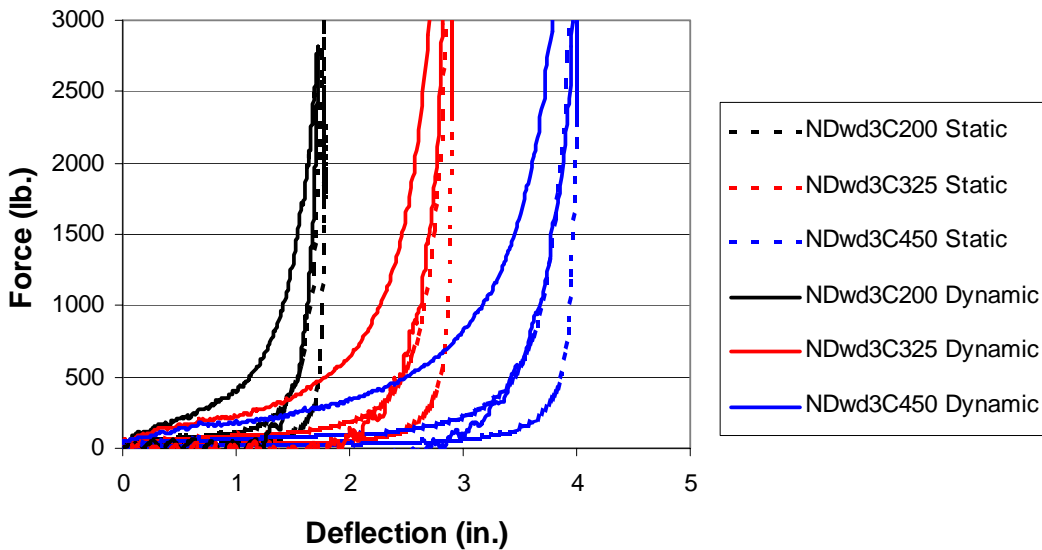
FIGURE 3-31. STATIC AND DYNAMIC TEST RESULTS FOR NDwd3

Static tests were also conducted on the laminated flotation specimens. The results of these tests are presented in figures 3-32 through 3-34.
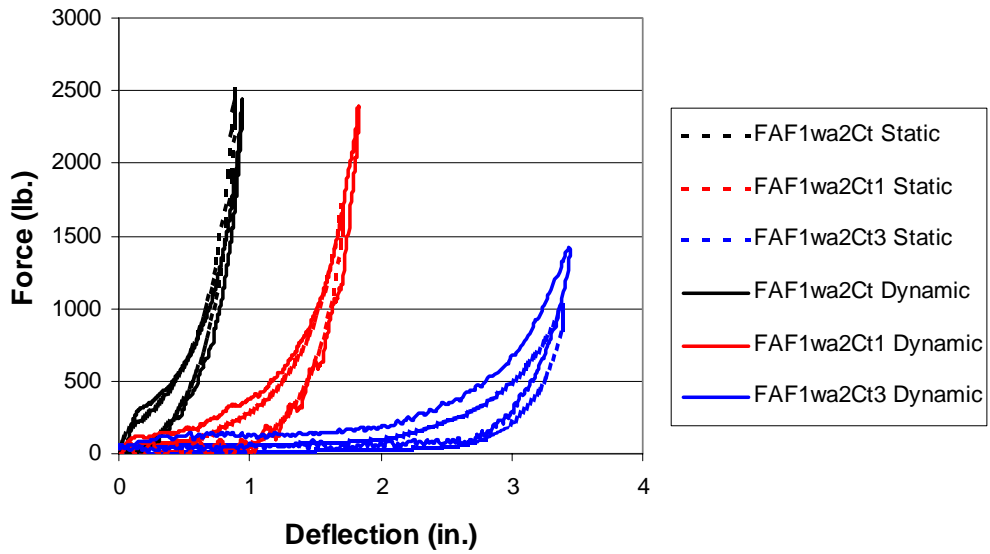
FIGURE 3-32. STATIC AND DYNAMIC TEST RESULTS FOR FAF1wa2
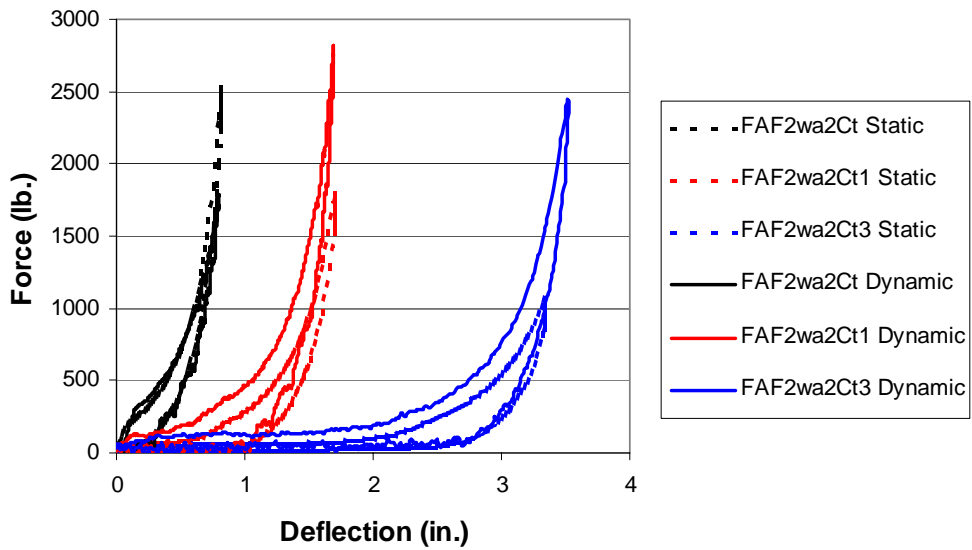
FIGURE 3-33. STATIC AND DYNAMIC TEST RESULTS FOR FAF2wa2
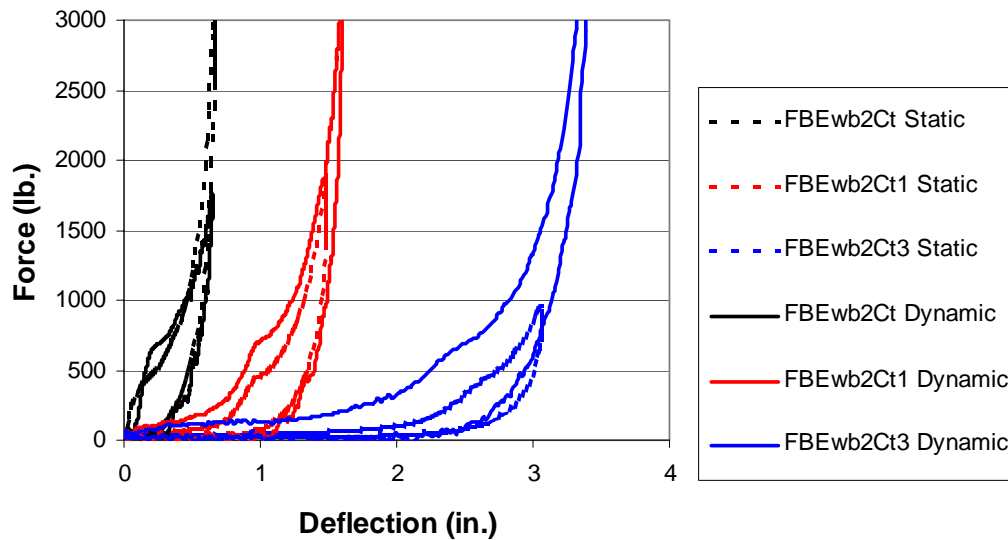
FIGURE 3-34. STATIC AND DYNAMIC TEST RESULTS FOR FBEwb2

CF-42 pink CONFOR foam was tested statically and dynamically. CONFOR is recognized as a rate-sensitive foam and, thus, can serve as a benchmark to determine the degree to which a foam exhibits significant rate properties. It is available in a number of densities, with CF-42 being one of the softer of these. The results of the tests for 2-, 3 1/4-, and 4 1/2-in. CF-42 specimens are presented in figure 3-35. Note the much greater difference in the dynamic-to-static strengths for this material compared to the results for the other materials presented in figures 3-29 through 3-34.
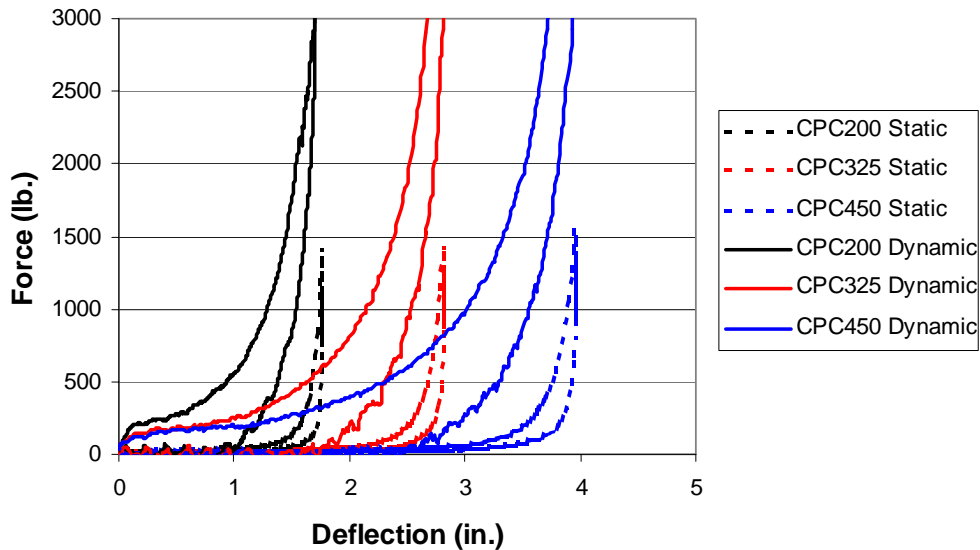
FIGURE 3-35. STATIC VS DYNAMIC COMPARISON FOR CONFOR CF-42

3-19

Component tests were also conducted on the rectangular seat cushions to investigate the differences between the responses produced by these specimens and those produced by standard cylindrical specimens. The nonflotation cushion test results are presented in figures 3-36 through 3-41.
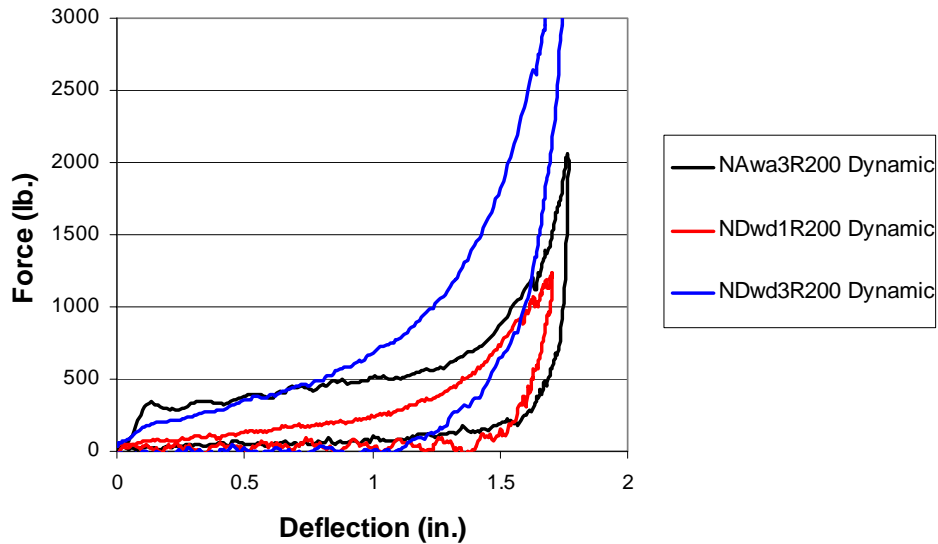
FIGURE 3-36. LOAD-DEFLECTION CURVES FOR 2-in. NONFLOTATION CUSHIONS
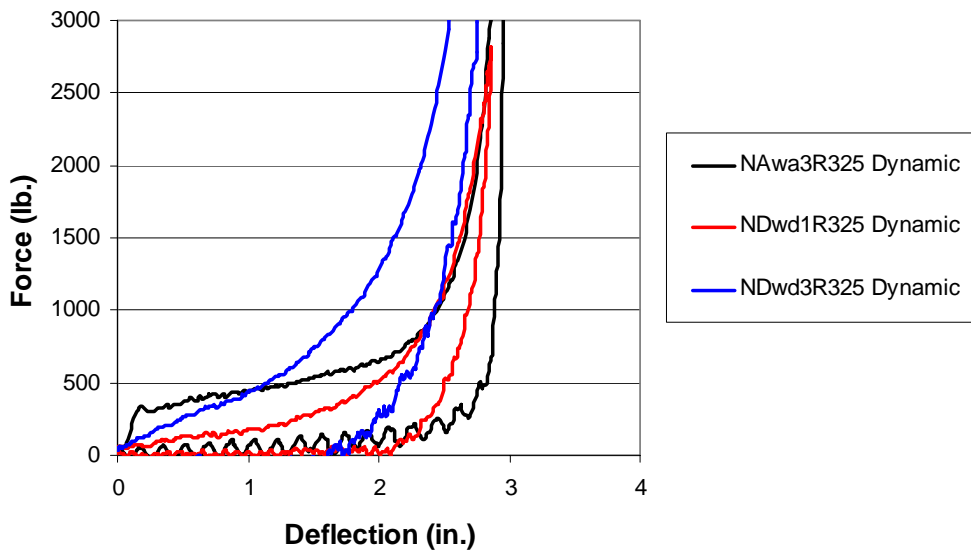
FIGURE 3-37. LOAD-DEFLECTION CURVES FOR 3 1/4-in. NONFLOTATION CUSHIONS
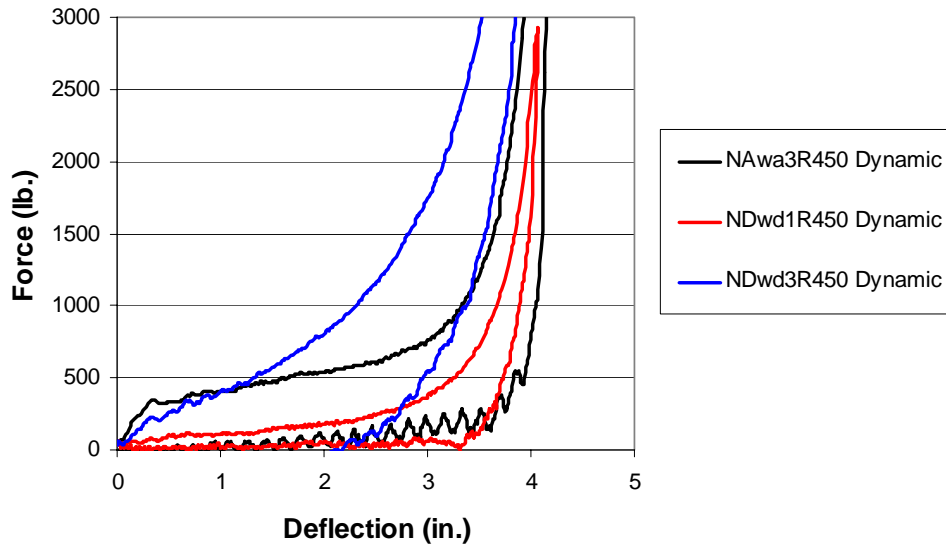
FIGURE 3-38. LOAD-DEFLECTION CURVES FOR 4 1/2-in. NONFLOTATION CUSHIONS
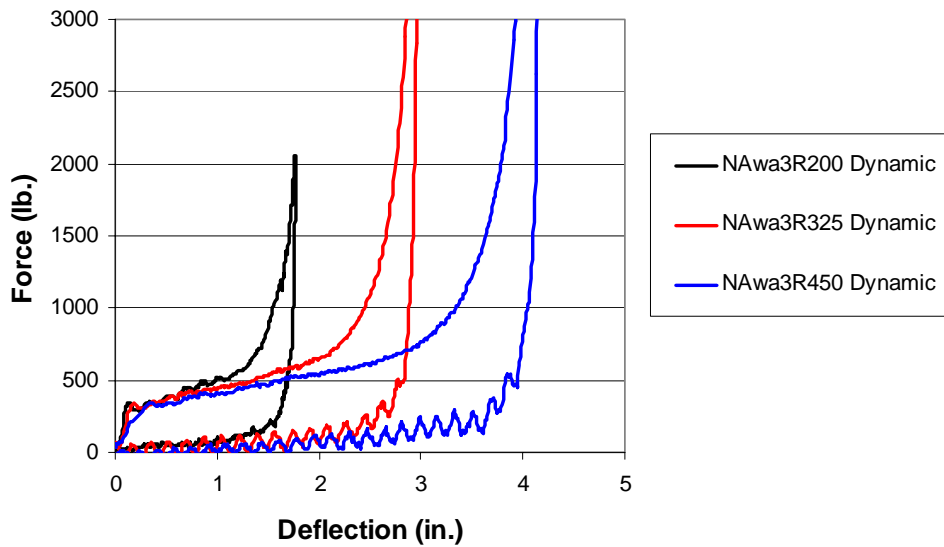
FIGURE 3-39. LOAD-DEFLECTION CURVES FOR VARIOUS CUSHION
THICKNESSES FOR NAwa3
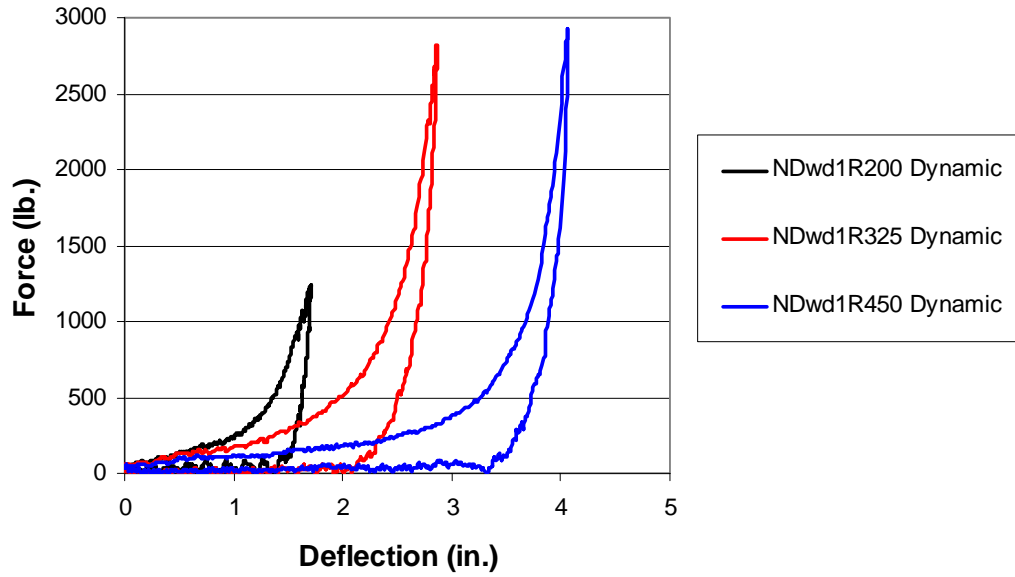
FIGURE 3-40. LOAD-DEFLECTION CURVES FOR VARIOUS CUSHION
THICKNESSES FOR NDwd1
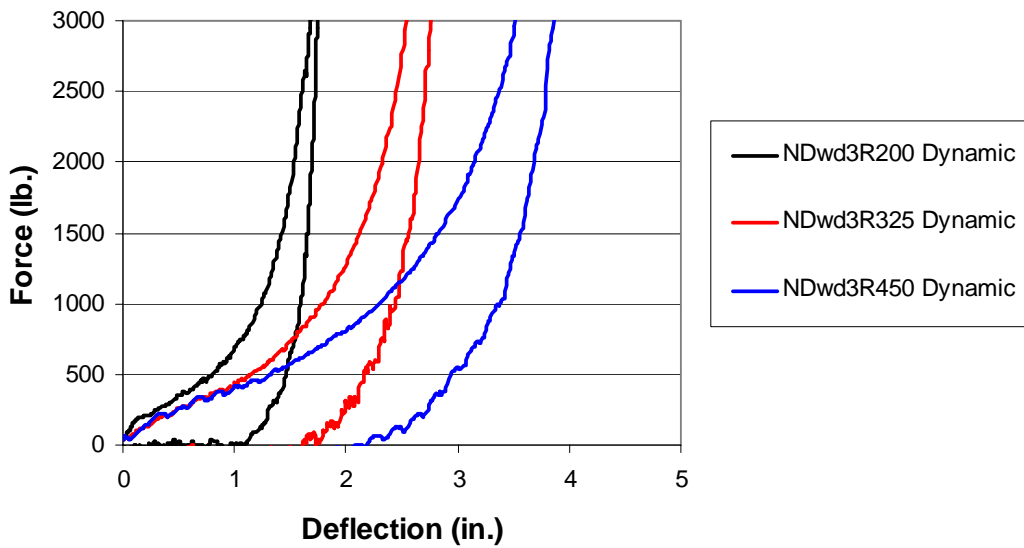
FIGURE 3-41. LOAD-DEFLECTION CURVES FOR VARIOUS CUSHION
THICKNESSES FOR NDwd3

Dynamic component tests were also conducted on rectangular flotation cushions. The results are presented in figures 3-42 through 3-47.
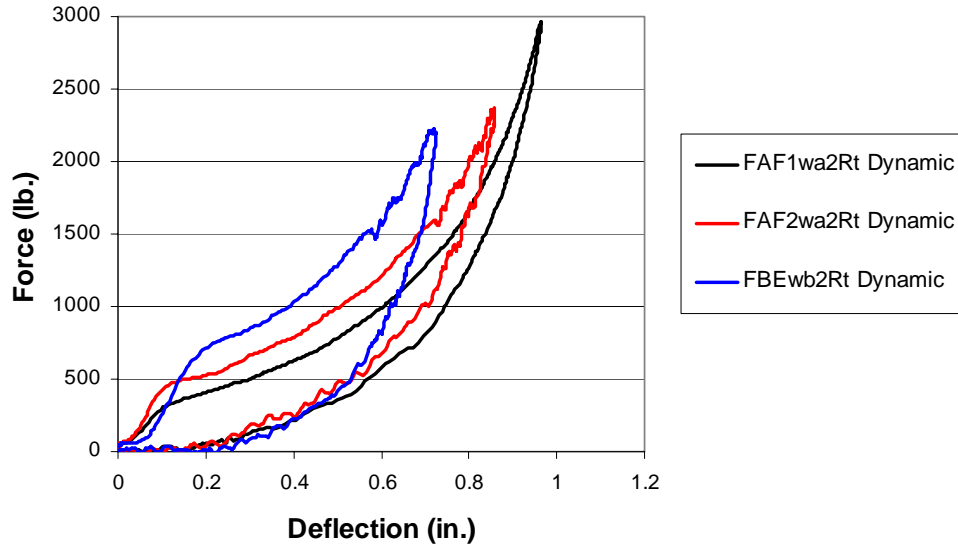
FIGURE 3-42. LOAD-DEFLECTION CURVES FOR LAMINATED 1-in.
FLOTATION CUSHIONS
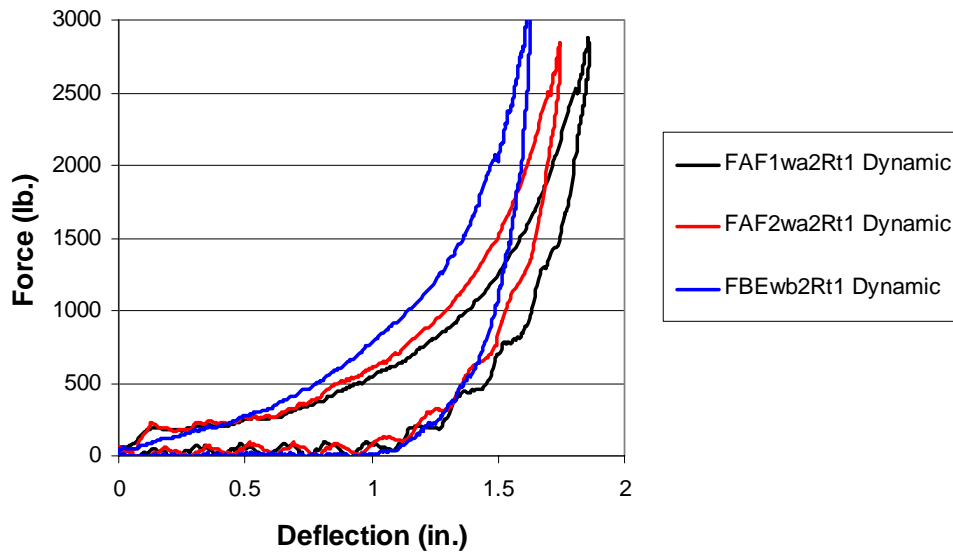
FIGURE 3-43. LOAD-DEFLECTION CURVES FOR LAMINATED 2-in.
FLOTATION CUSHIONS
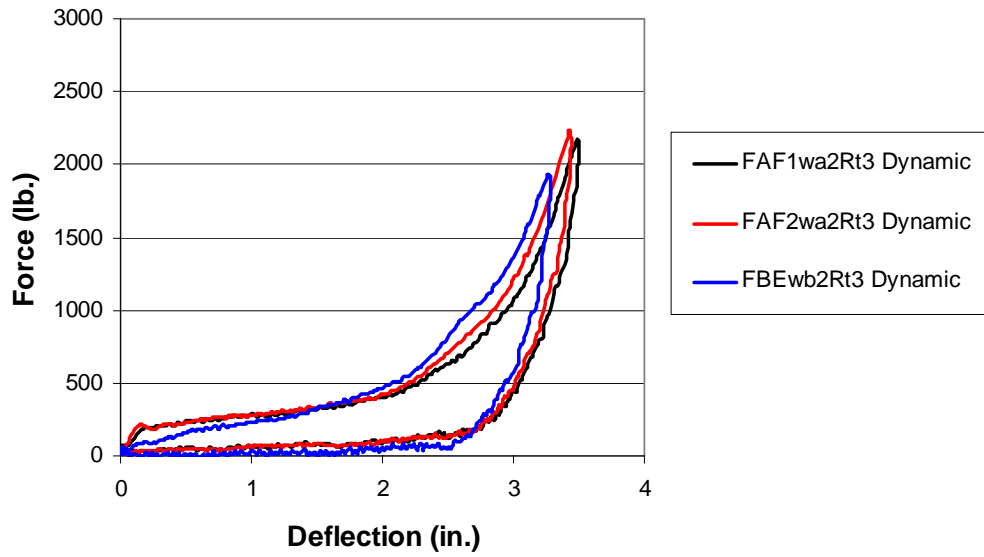
FIGURE 3-44. LOAD-DEFLECTION CURVES FOR LAMINATED 4-in.
FLOTATION CUSHIONS
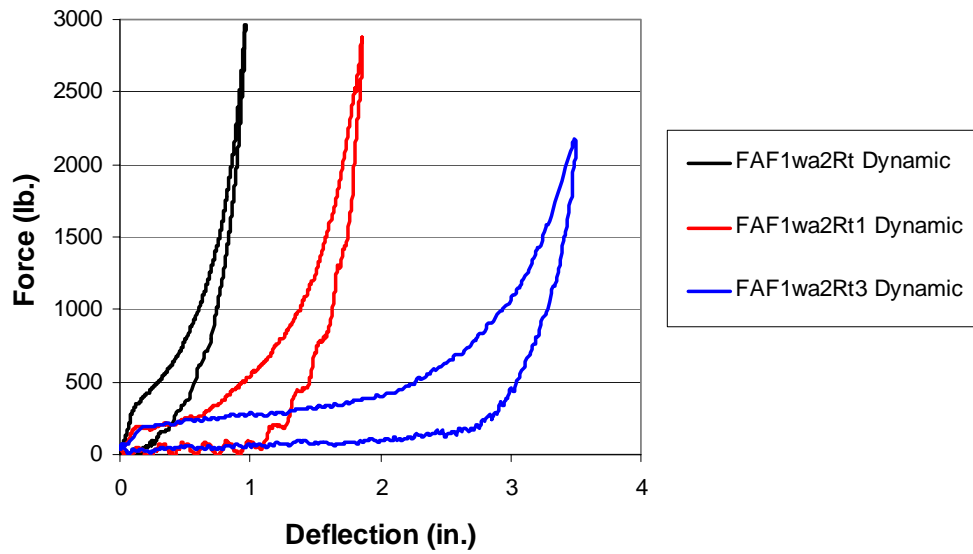
FIGURE 3-45. LOAD-DEFLECTION CURVES FOR FAF1wa2
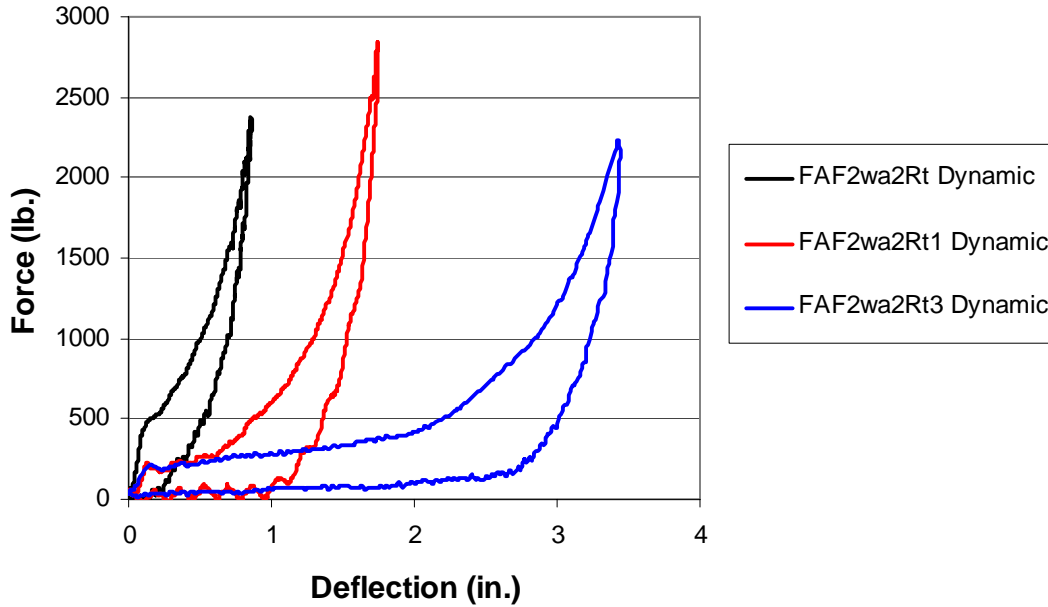
FIGURE 3-46. LOAD-DEFLECTION CURVES FOR FAF2wa2
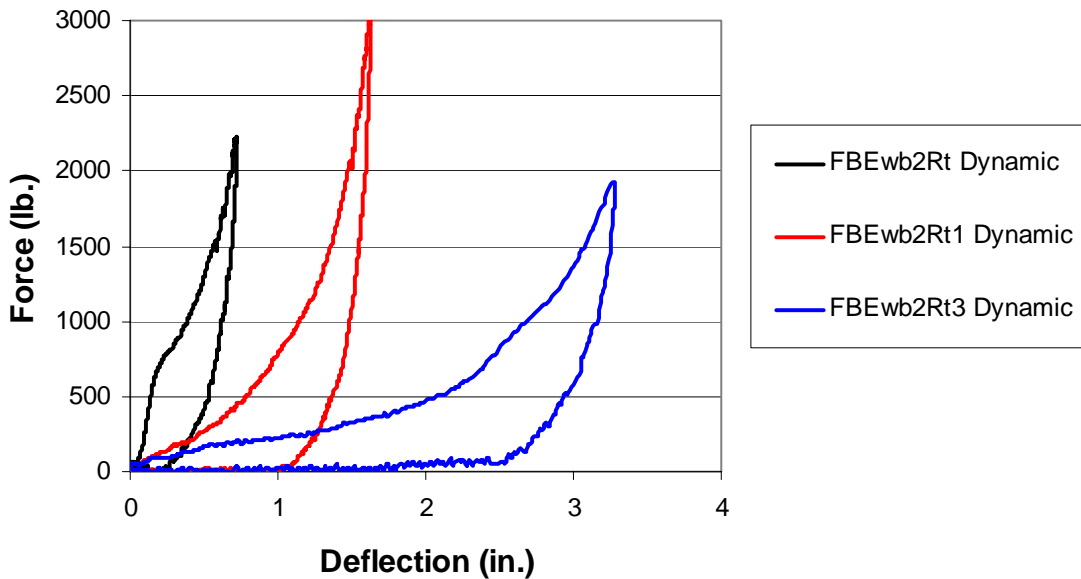
FIGURE 3-47. LOAD-DEFLECTION CURVES FOR FBEwb2

Dynamic material tests were conducted for both cylindrical and rectangular cushion specimens to gain insight into the behavior of typical foam materials. One-dimensional stress-strain data are often used to model foam materials, and the cylindrical specimen tests can be thought of as this kind of one-dimensional problem. The rectangular specimen tests, on the other hand, clearly represent a three-dimensional boundary problem. Examining these data, it is seen that the data for the rectangular specimens reflects a stronger material than that obtained during the cylinder tests. This difference is a measure of foam materials to transfer shear forces through the material

and, as such, provides a measure of the differences between a one-dimensional boundary value problem and a multidimensional boundary value problem. The differences between the test results for the cylindrical and rectangular specimens are evident in figures 3-48 through 3-53.
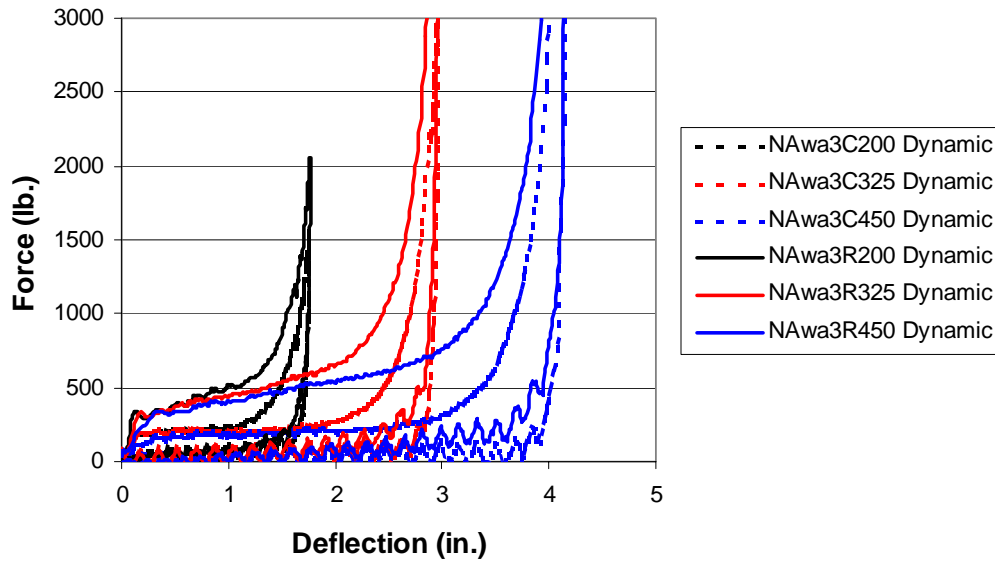
FIGURE 3-48. COMPARISON OF CYLINDRICAL AND RECTANGULAR RESPONSES FOR NAwa3
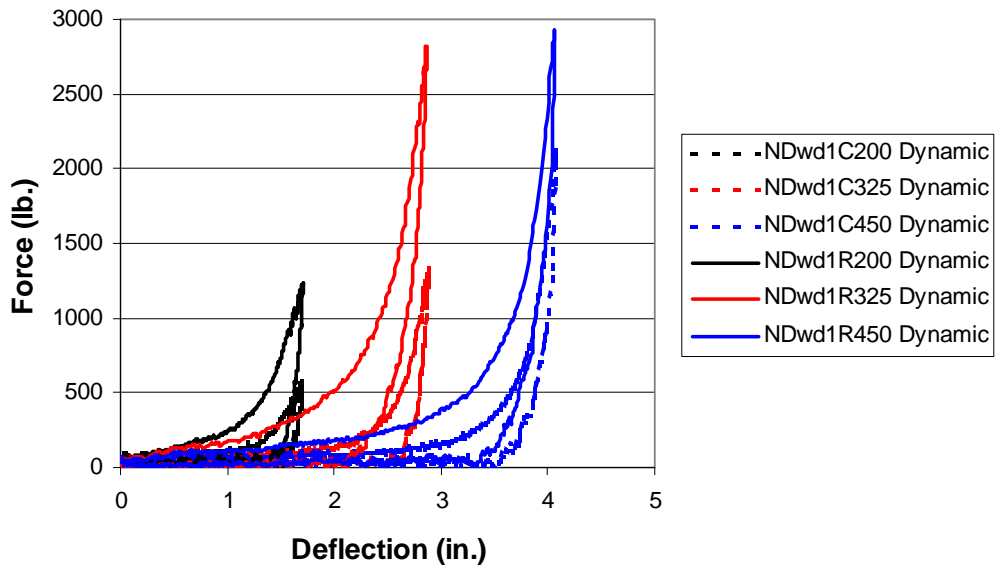
FIGURE 3-49. COMPARISON OF CYLINDRICAL AND RECTANGULAR RESPONSES FOR NDwd1
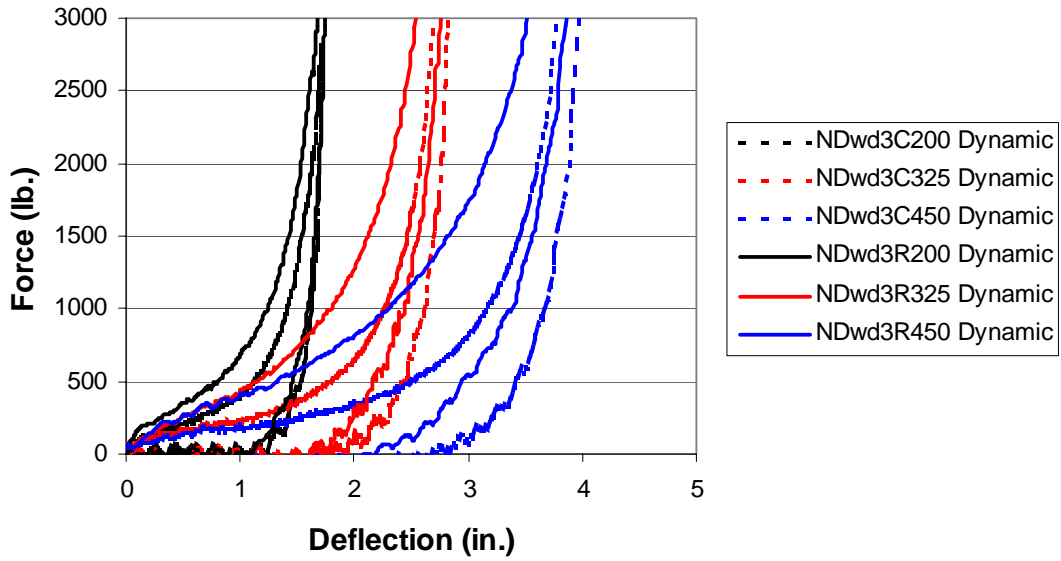
FIGURE 3-50. COMPARISON OF CYLINDRICAL AND RECTANGULAR
RESPONSES FOR NDwd3
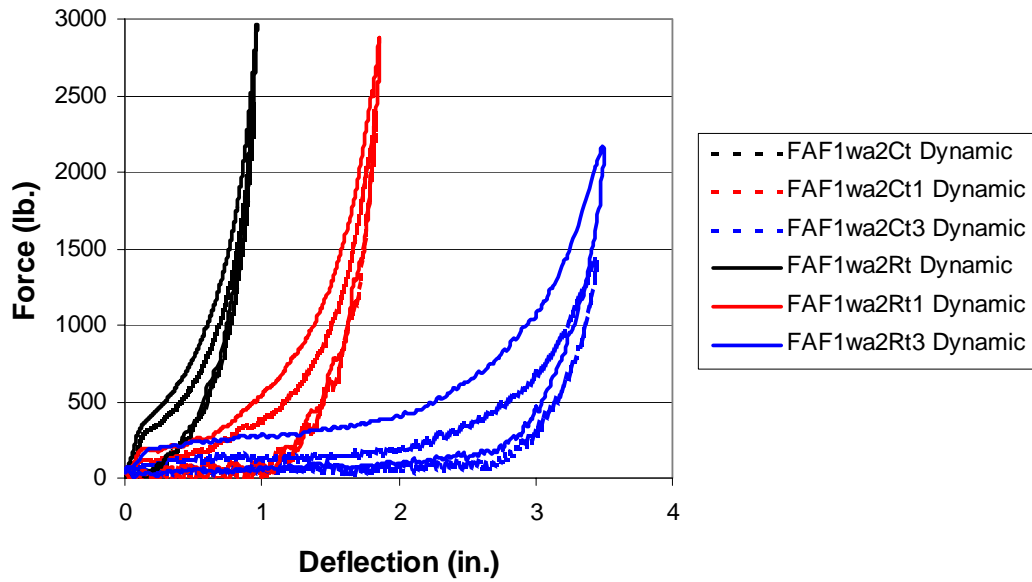
FIGURE 3-51. COMPARISON OF CYLINDRICAL AND RECTANGULAR
RESPONSES FOR FAF1wa2
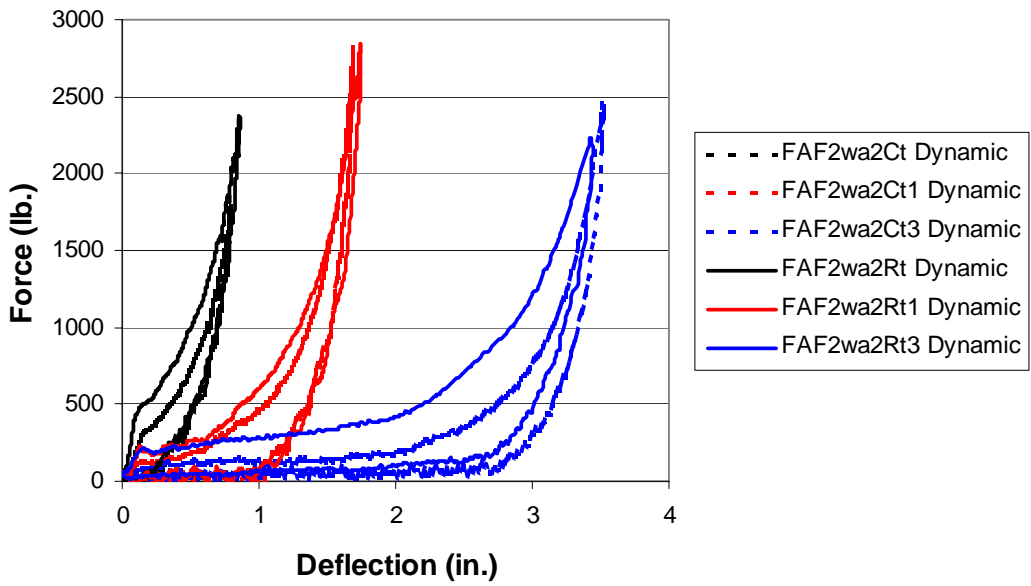
FIGURE 3-52. COMPARISON OF CYLINDRICAL AND RECTANGULAR
RESPONSES FOR FAF2wa2
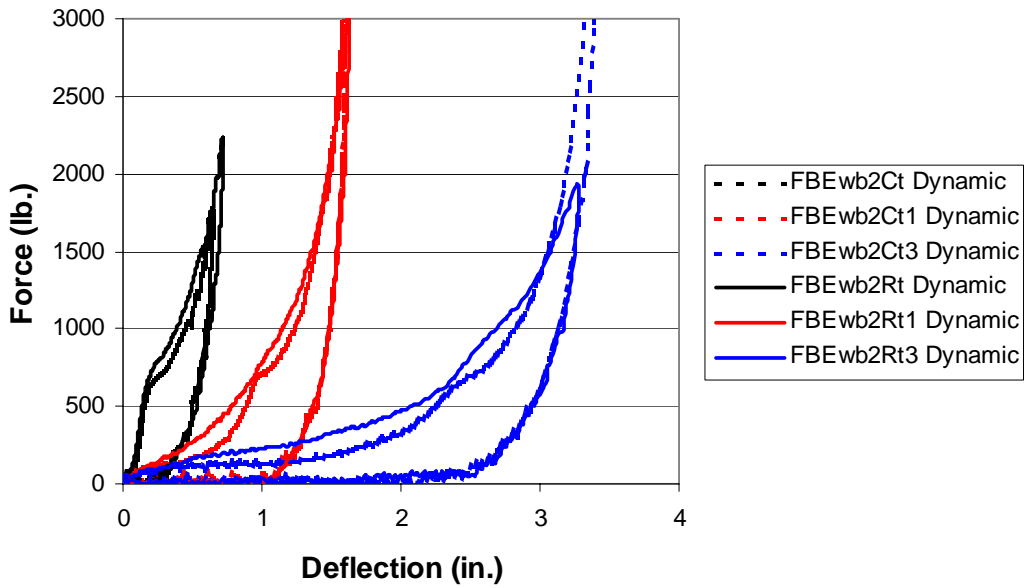
FIGURE 3-53. COMPARISON OF CYLINDRICAL AND RECTANGULAR
RESPONSES FOR FBEwb2

The criterion force-deflection curve was determined for the nonflotation cushions by performing a series of regression analyses along the family of curves as shown in figures 3-54 and 3-55. In these figures, $\overline{F}$ represents nondimensional force, which is defined as the force divided by the maximum force, and $\overline{\delta}$ represents nondimensional deflection, which is defined as the deflection divided by the maximum deflection. Note, the data presented in these figures are illustrative; it is not test data.
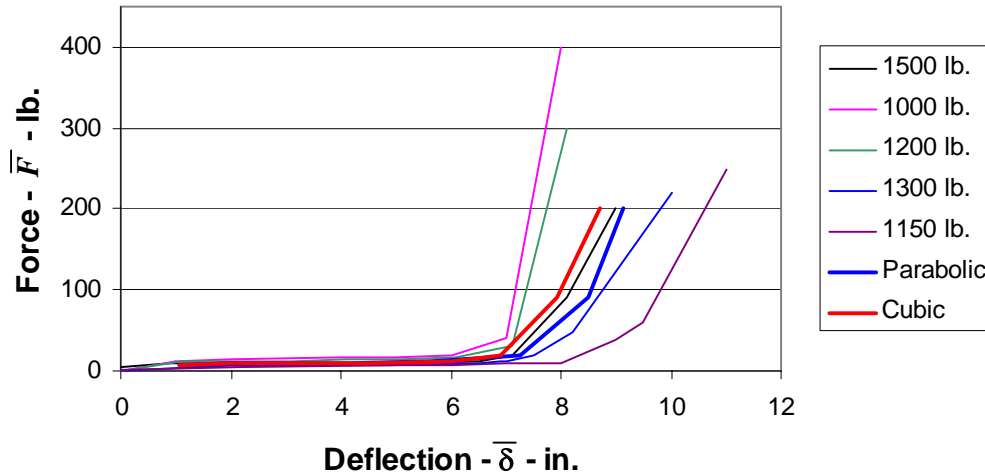
FIGURE 3-54. TYPICAL REGRESSION ANALYSIS RESULTS—EXAMPLE 1
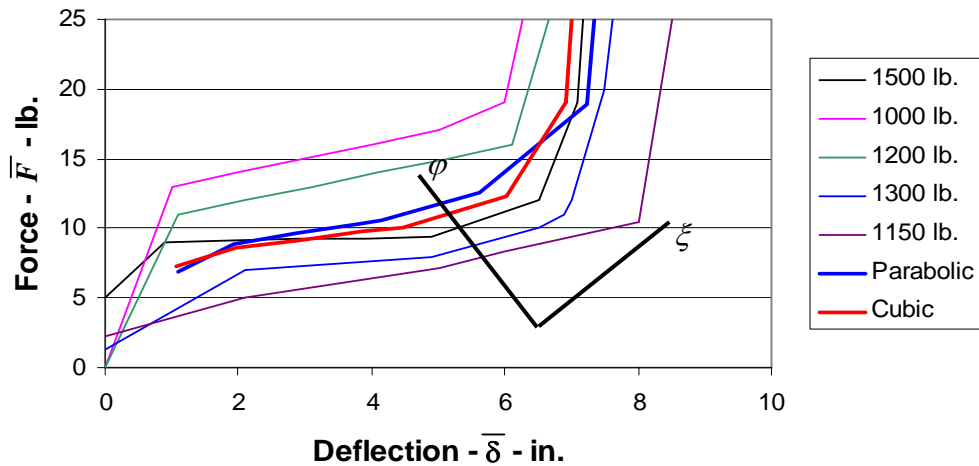
FIGURE 3-55. TYPICAL REGRESSION ANALYSIS RESULTS—EXAMPLE 2

The regression analyses determined the locations of two curves, which maximize the lumbar load at each point along the pseudocriterion curve. The pseudocriterion curve is defined as the curve associated with the maximum lumbar load measured during the dynamic cushion tests. Thus, in this example, the pseudocriterion curve is associated with the 1500-lb curve. The regression analysis determined the location of the maximum lumbar load along the φ axis, as shown in figure 3-55. Therefore, the ξ–φ coordinate system is defined with the ξ axis bisecting

the angle formed by the two adjacent line segments on the pseudocriterion curve. The φ_i coordinates for each of the load deflection curves are now conveniently determined by a simple linear interpolation of the form

$$\varphi_j = \varphi_j\left(\xi_i\right) \tag{3-1}$$

where ξ and φ = computational coordinates representing transformed nondimensional force-deflection data.

where the subscripts refer to the ith point and the jth curve. The transformation to the $\xi-\varphi$ computational coordinates is conveniently computed as

$$\begin{Bmatrix} \xi \\ \varphi \end{Bmatrix} = \begin{bmatrix} \cos\theta & \sin\theta \\ -\sin\theta & \cos\theta \end{bmatrix} \begin{Bmatrix} d \\ F \end{Bmatrix} \tag{3-2}$$

which is also written as

$$\begin{Bmatrix} \xi \\ \varphi \end{Bmatrix} = \begin{bmatrix} T \end{bmatrix} \begin{Bmatrix} d \\ F \end{Bmatrix} \tag{3-3}$$

where:

T = transformation matrix relating ξ and φ to nondimensional force-deflection data
d = cushion depth (in.)
F = force (lb)

The lumbar loads for each of the cushions can now be plotted versus φ and a quadratic curve fit to the data, as shown in figure 3-56.

$$P = -32.537\varphi^2 + 440.01\varphi - 2.8138$$
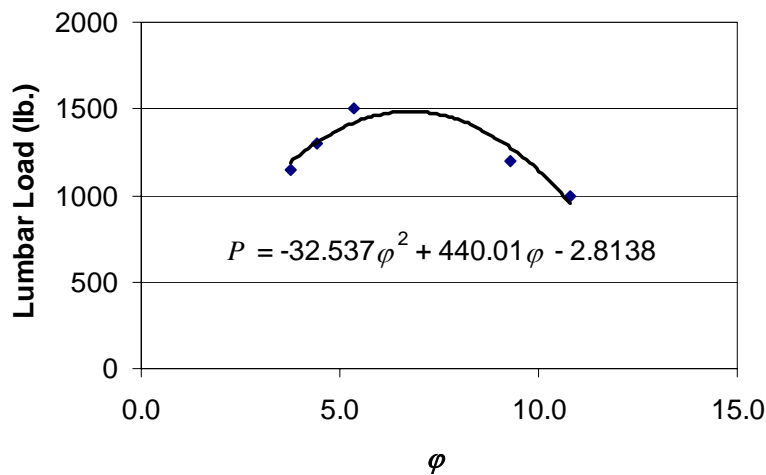
FIGURE 3-56. QUADRATIC REGRESSION

3-30

A cubic regression was also performed, as shown in figure 3-57.
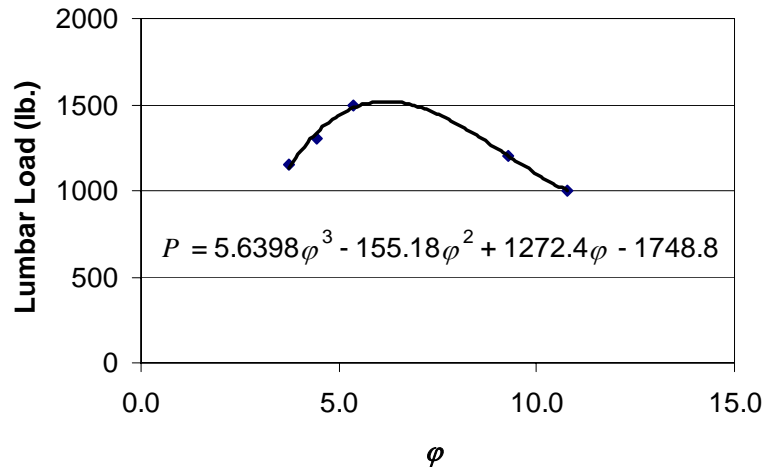
FIGURE 3-57. CUBIC REGRESSION

The location of the maximum lumbar load φ^* can now be determined by the following

$$P = \sum_{i=0}^{N} a_i \, \varphi^i \tag{3-4}$$

$$\frac{dP(\varphi^*)}{d\varphi} = \sum_{i=1}^{N} i \, a_i \, \varphi^{i-1} = 0 \tag{3-5}$$

For the quadratic case, this equation yields

$$2 \, a_2 \, \varphi^* + a_1 = 0 \tag{3-6}$$

The cubic case yields a similar equation

$$3 \, a_3 \left(\varphi^*\right)^2 + 2 \, a_2 \, \varphi^* + a_1 = 0 \tag{3-7}$$

Recalling that

$$\xi^* = \xi_i = \text{ constant} \tag{3-8}$$

These equations are solved for φ^*, and the location of the corresponding point on material load-deflection curve is subsequently computed as

$$\left\{ \begin{array}{c} d^* \\ F^* \end{array} \right\} = [T]^T \left\{ \begin{array}{c} \xi^* \\ \varphi^* \end{array} \right\} \tag{3-9}$$

The criterion curve is represented as the curve passing through the loci of the points (ξ^*, φ^*). The cushion force-deflection data was nondimensionalized for numerical implementation of this analysis by dividing the force and deflection data by the largest force and largest displacement, respectively. The results of the quadratic and cubic regression analyses for the 4 1/2-in. nonflotation cushion materials are compared in figure 3-58.
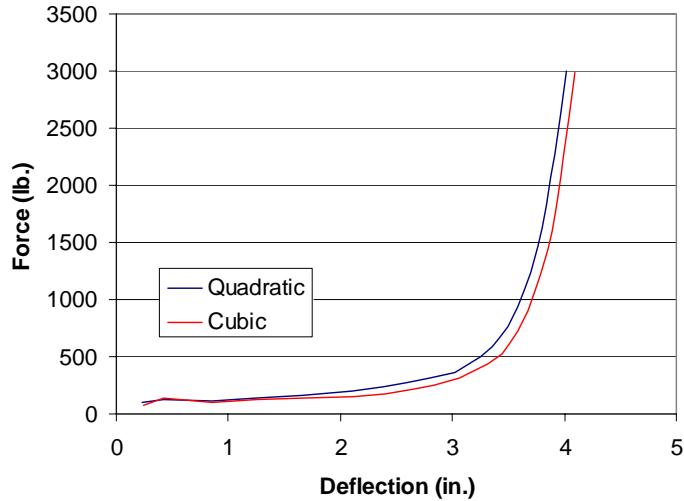
FIGURE 3-58. REGRESSION COMPARISON

The goodness of the regressions are assessed in figures 3-59 through 3-61, which represent section cuts through the data. The first of these represents the data at the beginning of the load-deflection curves. Note that the direction of the φ^* axis is reversed from that shown in figure 3-55.
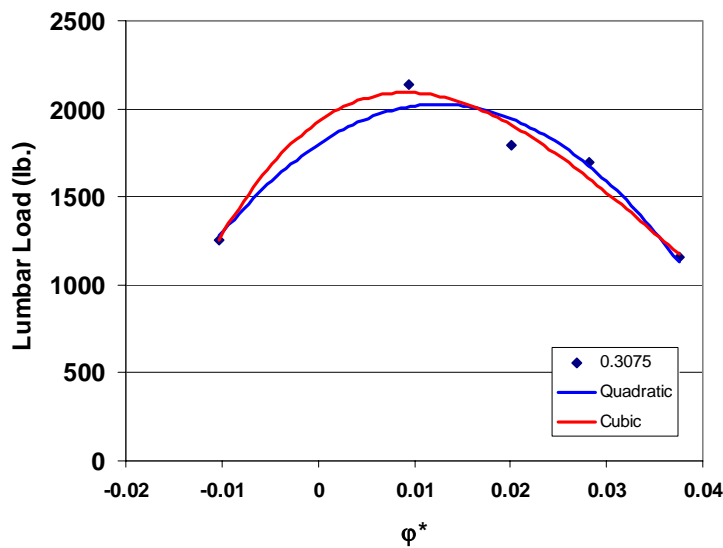
FIGURE 3-59. REGRESSIONS AT $x/x_{\max} = 0.3075$

A section cut near the center of the load deflection curve is shown in figure 3-60.
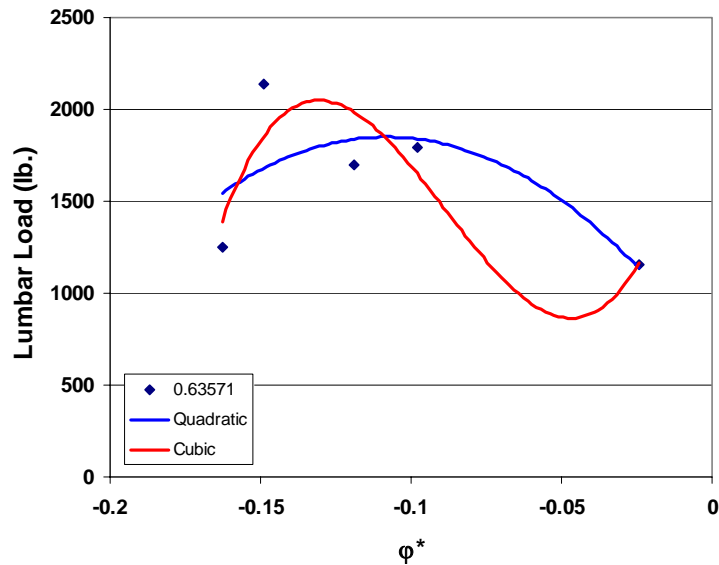
FIGURE 3-60. REGRESSIONS AT $x/x_{max} = 0.63571$

The final section cut shows the regressions in the densification region, which is at the right side of the load-deflection plots.
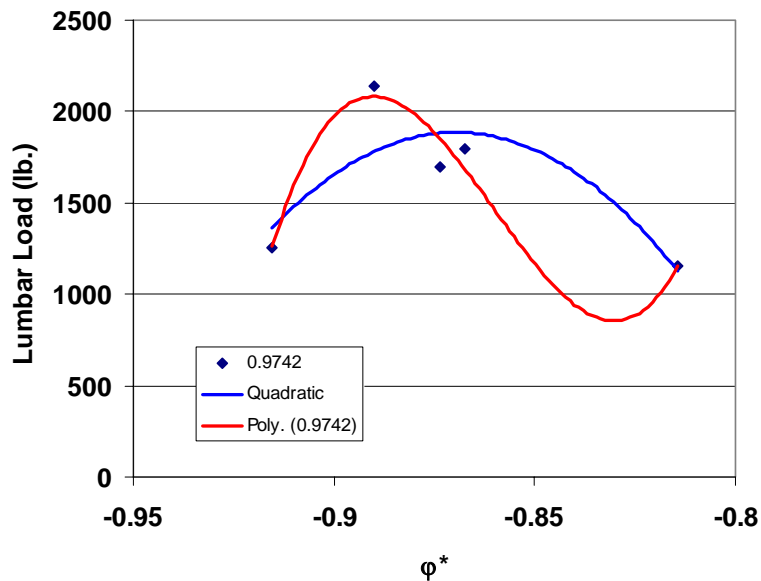
FIGURE 3-61. REGRESSIONS AT $x/x_{max} = 0.9742$

An examination of figures 3-59 through 3-61 show that the second data point from the left in these figures, NCwb2C450, does not fit these regressions as well as the other four points. This is not evident at the beginning of the load-deflection curve, but develops quickly and persists for

the remainder of the curve. This is evidence that another effect, not entirely reflected in the regression analysis, influences the lumbar load for this material. This data point has a greater affect on the cubic distribution than on the quadratic distribution. Fortunately, it does not produce a significant shift in the location of the maximum lumbar load, since the difference (along the displacement axis) between the criterion curves predicted by the quadratic and cubic regressions is less than the typical thickness tolerance for seat cushion. Nevertheless, the quadratic curve is judged to be the better fit of the data and is, thus, selected as the basis for the criterion curve.

A re-examination of the dynamic sled test data reveals that the static deflection for this cushion was significantly less than the static deflection for all of the other cushions. This could produce a significant increase in the lumbar load, as evidenced by the outlying data point shown in the figures 3-60 and 3-61.

This quadratic curve is superimposed on the experimental load-deflection curves in figure 3-62.
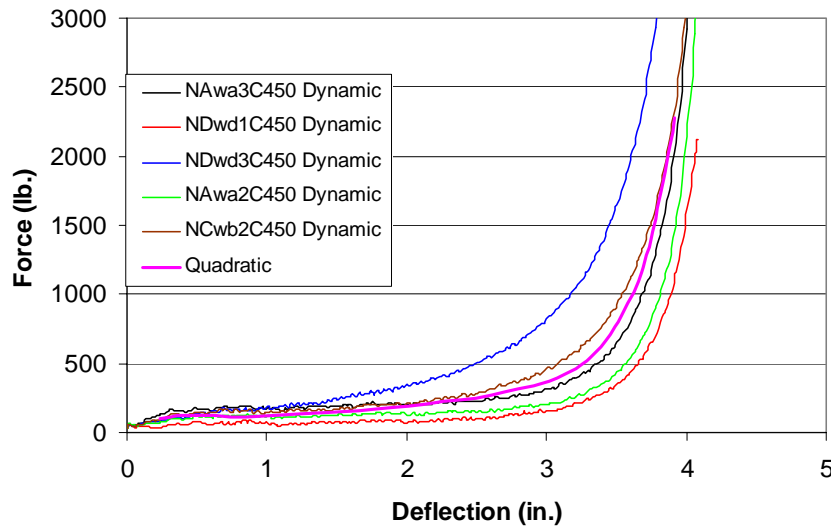
FIGURE 3-62. REGRESSION RESULTS, 4 1/2-in. NONFLOTATION FOAMS

3.6 DISCUSSION.

The load-deflection data presented above is consistent with the form described by Gibson and Ashby. The plateau and densification regions are obvious for all the materials, and the linear elastic region is evident during the initial response for most of them. The qualitative correlation of lumbar load with the cushion properties suggests the existence of a specific load-deflection curve that maximizes the lumbar load for a given cushion thickness. This means that the lumbar load associated with curves, either above or below the critical curve, will produce lower lumbar loads. It is also noted that for a given thickness of material, the densification strain (or displacement) decreases as the plateau strength increases. Conversely, the densification strain is also frequently observed to increase as the plateau strength decreases. The data presented in this

report clearly shows that the material response generated by a simple foam specimen is quite complicated and cannot be completely characterized by a two-point IFD test.

The results presented also point to the fact that one cannot assume that either the softest cushion, i.e., the cushion with the lowest IFD, or the firmest cushion, i.e., the cushion with the greatest IFD, will produce the greatest lumbar load.

The following mental experiment serves as a sanity test for this observation. A 14-g rigid, iron seat test dynamic download seat test (without a cushion), per 14 CFR 25.562(b)(1), produced a lumbar load well below 1000 lb. One might mentally plot the load-deflection curve for the iron seat and compare it with the cushion data presented in this report. Obviously, the load-deflection curve for a rigid seat lies above all the cushion data presented in this report. This leads to the hypothesis that the lumbar loads associated with the family of load-deflection curves above the criterion curve will asymptotically approach the rigid seat load, or about 1000 lb. This, too, is consistent with the data produced by this research.

As a second mental experiment, consider a very soft seat cushion that is placed on the iron seat. Imagine a cushion that is so soft that it is completely consolidated under the occupant's weight. Thus, this load-deflection curve lies below all the cushion data presented in this report. Recalling that a 1-g preload is imposed on the cushion before conducting a dynamic seat test and assuming that this will completely consolidate the extremely soft cushion, one can conclude that the post 1-g cushion/seat pan load-deflection curve will be nearly as stiff as the steel plate considered in the first mental experiment. Therefore, the lumbar load for this cushion will approach 1000 lb as well, thus implying that the lumbar loads associated with the family of load-deflection curves below the criterion curve will asymptotically approach the rigid seat load at or about 1000 lb.

A review of the results for the laminated cushions reveals that their responses contain both similarities and differences when compared to the results for the nonflotation cushions. The most obvious similarity is that the criterion curve for the laminated flotation cushions is similar to those for monolithic cushions. However, a significant difference lies in the fact that the laminated cushion criterion curve is positioned along one side of all the laminated cushion properties rather than in the middle of the data. This is consistent with the discussion presented above if one recognizes that the rigid layer of flotation foam will never generate the same kind of response as a very soft, very weak foam, i.e., the subject of the first mental experiment described above. Thus, all flotation cushions inherently behave in a manner that is similar to the force-deflection curves presented in figures 3-42 through 3-44. However, examining the flotation data presented in these figures, it is seen that the flotation criterion curve must lie below and to the right of the set of curves presented in these figures.

4. PROPOSED CUSHION REPLACEMENT METHODOLOGY.

The following method can be used to show that a replacement seat cushion satisfies the lumbar load injury criterion of 14 CFR 25.562 or TSO C-127A. This methodology requires that the replacement cushions possess the same thickness as the original cushions. The term "same thickness" refers to a comparison of the cushion thicknesses in the buttock reference point (BRP) region, (which is defined as the area 1 to 9 in. forward of the seat reference point (SRP) and ±7 in. on each side of the seat centerline). The difference between the thicknesses of the original and replacement cushions should differ by no more than 1/2 in. It is expected that a comparison of fore-aft section cuts is sufficient to evaluate this requirement. This method was developed for cushions whose load-deflection curves can be described by the functional form presented in figure 1-3. For example, the nonflotation cushion load-deflection curves presented in figures 3-1 through 3-3 all possess the same functional form, as do the load-deflection curves for the flotation cushions presented in figures 3-13 and 3-14.

The cushion replacement methodology is, in part, based on the fact that a criterion curve exists, which enables the cushion designer and the certification engineer to define and certify a replacement cushion that produces a lower lumbar load than the originally certified cushion. Note that this evaluation is based on the loading portion of the load-deflection curve. The unloading portion is not judged to be as critical for cushions constructed of materials of highly rate-sensitive materials or crushable materials. CONFOR is an example of a highly rate-sensitive material, and honeycomb or rigid-tooling foams are examples of crushable materials.

4.1 COMPONENT TEST METHOD.

This test is called the dynamic indentation force deflection test, and the results are called the dynamic force-deflection data. The test is appropriate for typical upholstery and flotation foams used in the construction of aircraft seat bottom cushions. The method is not intended for use in evaluating energy-absorbing seat cushion designs that use honeycomb, highly rate-sensitive foam, or rigid-tooling foam in their construction.

4.1.1 Specimen Definition.

The specimen shall consist of a 7 1/2-in.-diameter cylinder. The unloaded specimen thickness shall represent the unloaded cushion thickness at the position of the anthropomorphic test dummy (ATD) ischial tuberosity (BRP) when the dummy is placed in the seat. The BRP is located 4 1/2 in. forward of the SRP [22]. The specimens shall feature a similar type of material, i.e., fireblocking or muslin, as the certified seat cushion to be replaced.

4.1.2 Test Apparatus.

The test shall employ the perforated platten and foot described in ASTM D 3574, Test B_1 – Indentation Force Deflection Test-Specified Deflection. The foot shall be mounted on a hemispherical bearing. The platen (horizontal plate) shall be perforated with 1/4-in. holes on approximately 3/4-in. centers. It is suggested that the platen be reinforced as described in section 2.

4.1.3 Instrumentation.

Instrumentation shall include a force transducer appropriate for the measurement of dynamic force data, such as a pzieoresistive load cell or equivalent.

4.1.4 Pretest Measurements.

The following pretest measurements should be taken:

- Measure and record specimen thicknesses at points A-D, shown in figure 4-1.
- Measure and record specimen diameters A-B and C-D.
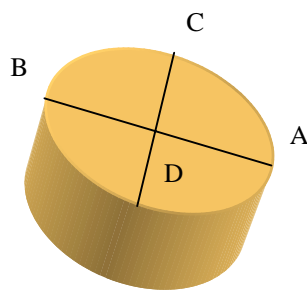
FIGURE 4-1. TEST SPECIMEN GEOMETRY

It is suggested that the test setup be photographed prior to the test.

4.1.5 Test Procedure.

The cushions and fixtures shall be maintained at a temperature between 66º to 78ºF for a minimum of 4 hours prior to and during the test. The cushions shall be maintained at a relative humidity of 10% to 70% for a minimum of 4 hours prior to and during the test.

The specimen shall be centered under the foot which shall be raised (or lowered) to be nearly in contact with the surface of the specimen. Note that the specimens are not to be preflexed as required by ASTM D 3574 since this may damage flotation cushions.

The load cells shall be zeroed (or a tare reading recorded) just prior to the test.

The specimen shall be loaded in compression, under displacement control, at a loading rate of approximately 27-33 in./sec to a maximum deflection corresponding to a $\frac{\Delta L}{L}$ of 0.9 (or the maximum value achievable without risking damage to the test stand and instrumentation). The ideal loading curve is shown in figure 4-2, where τ represents the nondimensional time required to load and unload the specimen. L represents the original specimen thickness and ΔL represents the change in thickness, or ram displacement.
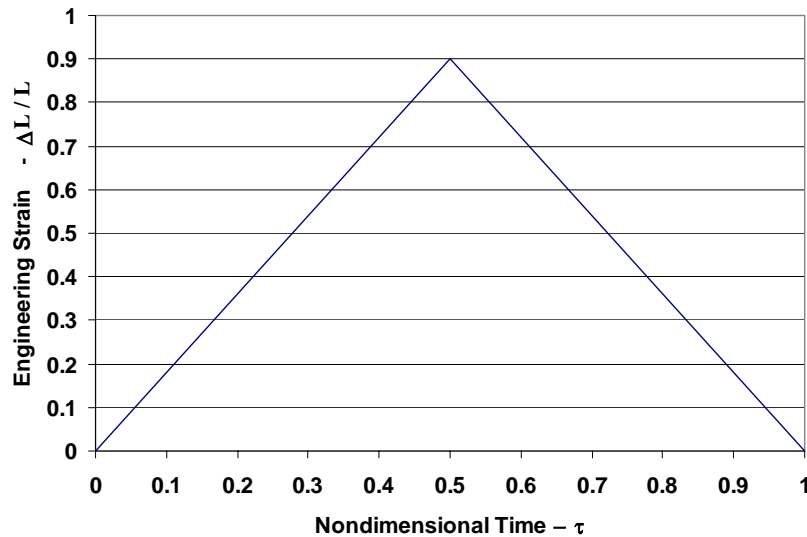
FIGURE 4-2. COMPONENT TEST LOADING IMPULSE

where

$$\tau = \frac{t}{t_{total}} \qquad (4\text{-}1)$$

Force and deflection data shall be recorded at a minimum sampling rate of 10,000 samples per second. Posttest filtering is not required.

4.2 APPLICATION TO MONOLITHIC (NONFLOTATION) CUSHIONS.

The component test for monolithic nonflotation seat cushions is described as follows:

- Fabricate specimens per section 4.1.1.

- Perform a component cushion test of the original certified cushion material and the proposed replacement cushion material per the procedures described in section 4.1.5. The material specimen should represent the cushion material and geometry.

- Compute the load-deflection criterion curve for the original certified cushion thickness at the BRP (using equations 1-9 and 1-10, and the loading portion of the stress-strain data for the nonflotation criterion curve presented in figure B-1 and table B-1 in appendix B). Typical results for cushions with thicknesses ranging from 2 to 5 inches are presented in figure 4-3 and table 4-1 to validate these calculations.
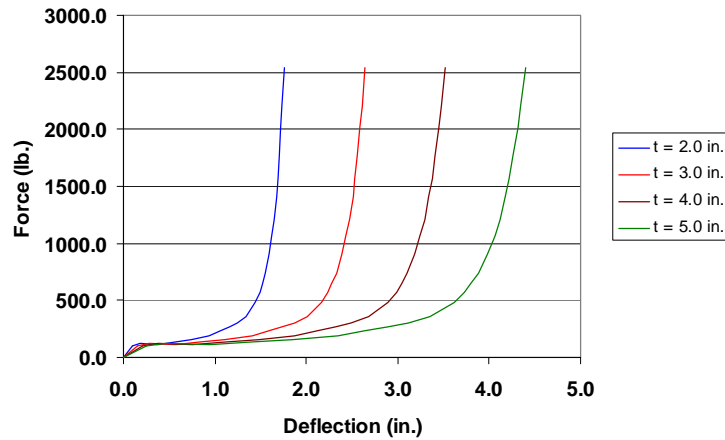
FIGURE 4-3. NONFLOTATION CRITERION CURVES ($A = 44.18$ in^2)

TABLE 4-1. CRITERION DATA, NONFLOTATION CUSHIONS ($A = 44.18$ in^2)

P (lb)	δ_2 (in.)	δ_3 (in.)	δ_4 (in.)	δ_5 (in.)
0.0	0.000	0.000	0.000	0.000
101.4	0.102	0.153	0.204	0.255
123.1	0.186	0.280	0.373	0.466
114.9	0.379	0.568	0.758	0.947
128.7	0.552	0.828	1.104	1.380
158.8	0.737	1.105	1.474	1.842
195.6	0.938	1.407	1.876	2.346
230.6	1.058	1.587	2.117	2.646
263.1	1.157	1.736	2.314	2.893
304.7	1.243	1.865	2.486	3.108
356.6	1.342	2.013	2.684	3.355
485.9	1.445	2.168	2.891	3.613
566.1	1.494	2.240	2.987	3.734
643.9	1.522	2.283	3.044	3.805
742.5	1.553	2.329	3.105	3.882
905.6	1.593	2.390	3.187	3.983
1065.0	1.623	2.435	3.247	4.058
1207.6	1.646	2.469	3.292	4.115
1414.8	1.672	2.508	3.344	4.180
1572.7	1.687	2.531	3.375	4.218
1772.4	1.706	2.558	3.411	4.264
2017.0	1.725	2.587	3.450	4.312
2206.9	1.738	2.607	3.475	4.344
2542.8	1.760	2.640	3.520	4.401

The nonflotation data are also tabulated in table 4-1, where δ_i denotes the deflection for a cushion of thickness i (i = 2, 3, 4, and 5 in.).

The performance requirements are as follows.

1.   If the original load-deflection curve possesses a greater plateau strength than the criterion curve, as shown in figure 4-4, then the replacement cushion must possess a strength equal to or greater than the original cushion material at all points in the Evaluation Region defined in figure 4-5. Thus, the Usable Region is defined as the area above the load-deflection curve for the certified cushion. Note that the loading portion of the material response is used to determine the relative position of the certified cushion curve relative to the criterion curve.
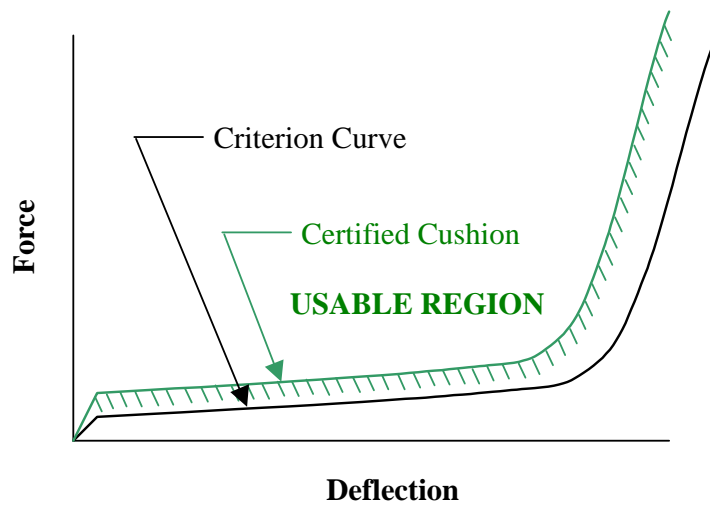
FIGURE 4-4. CASE 1, PLATEAU STRENGTH EXCEEDS CRITERION STRENGTH
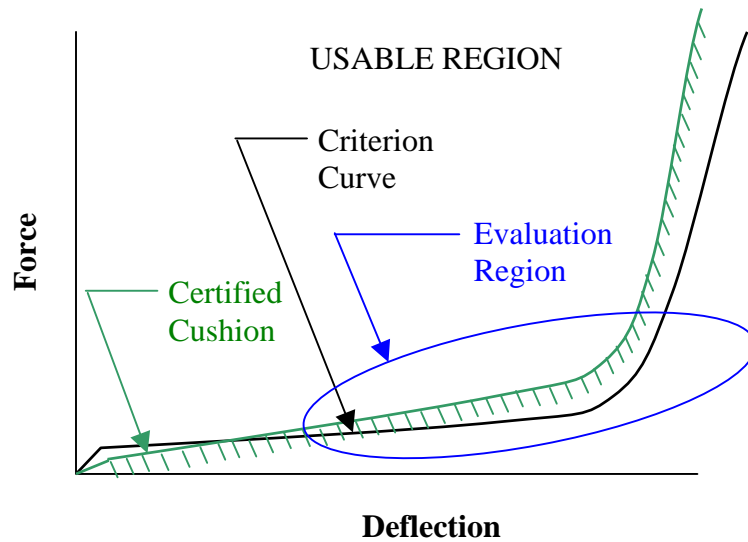
FIGURE 4-5. DEFINITION OF THE EVALUATION REGION

2.   If the original load-deflection curve possesses a lesser plateau strength than the criterion curve in the evaluation region, as shown in figure 4-6, then the replacement cushion must possess a strength equal to or lesser than the original cushion material for all points in the evaluation region.
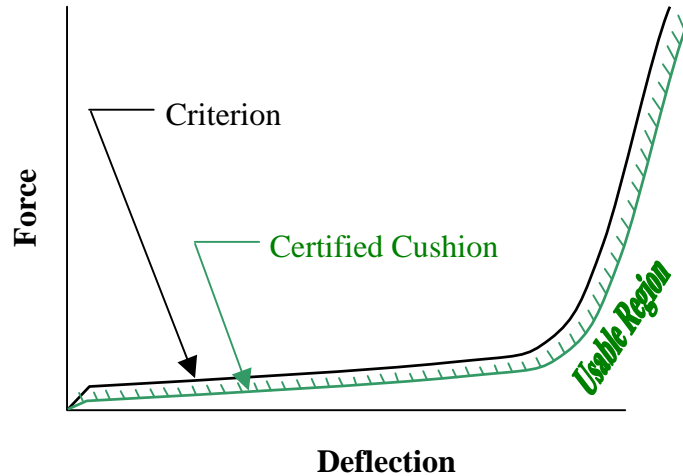
FIGURE 4-6. CASE 2, CRITERION STRENGTH EXCEEDS PLATEAU STRENGTH

3.   The determination of whether a specific data set should be analyzed as Case 1 or Case 2 depends on the data in the evaluation region of the load deflection curve shown in figure 4-6. The initial portion of the load-deflection curve controls the 1-g preload position, which is known to have a significant affect on the dynamic seat performance. The dynamic performance of a seat cushion is also sensitive to the latter part of the plateau strength region, i.e., the portion just preceding the densification region. Thus, the relative positions of the force-deflection curve and the criterion curve in the evaluation region are used to determine whether the plateau strength of the original certified cushion is above or below the criterion curve. Note also that the densification displacement of the certified cushion is less than densification displacement of the criterion curve when the plateau strength of the certified cushion is greater than the plateau strength of the criterion curve. Conversely, when the plateau strength of the certified cushion is less than the strength of the criterion curve, then the densification displacement of the certified cushion is greater than the criterion curve.

The compliance methodology described in this report cannot be applied to cushions possessing a force-deflection curve such as illustrated in figure 4-7. This material is identified as one where the load-deflection for the test data intersects the criterion curve in the densification region. (An intersection of these curves during the first 1/2 of the load-deflection curve is not a problem.) This kind of behavior was not observed during this research and may not exist. However, if it is encountered, further research is required to develop an appropriate evaluation methodology for these materials.
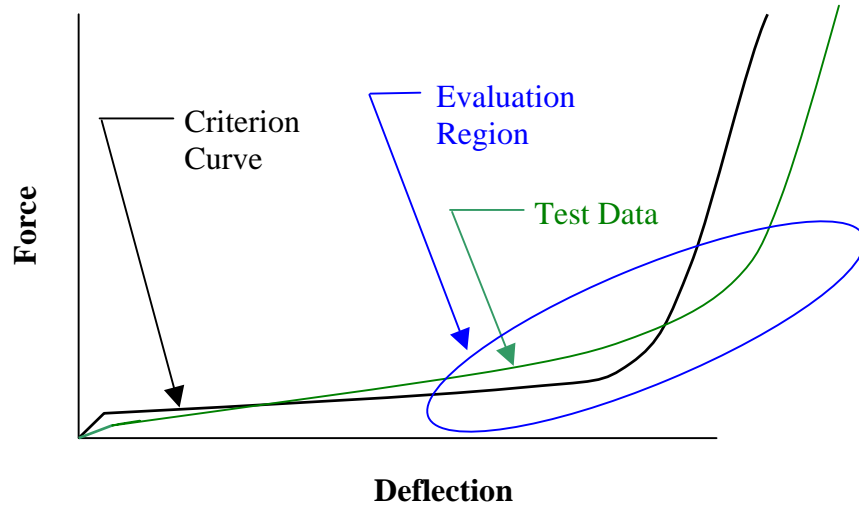
FIGURE 4-7. INELIGIBLE MATERIAL

4.   The deflection of the proposed cushion must be greater than or equal to the deflection of the certified cushion when subjected to a 1-g static preload, which is imposed by placing a 50th percentile male ATD on the cushion. This criterion is necessary because the component test evaluates the plateau strength region of the material response, not the initial response. The static performance may be evaluated by comparing the deflections at the SRP positions by placing an ATD on the cushions or by comparing the static deflections of component specimens produced by a 130-lb uniformly distributed static load using the component test fixture.

4.3 APPLICATION TO LAMINATED (FLOTATION) CUSHIONS.

The research results for laminated flotation seat cushions did not lead to a robust component test methodology. Therefore, additional tests and analyses are required before the method can be extended to these cushions.

5. CONCLUSIONS.

A qualitative correlation of lumbar load data generated during dynamic sled tests at the Civil Aerospace Medical Institute with dynamic load-deflection properties generated during material tests at Wichita State University shows that a critical load-deflection curve can be identified for monolithic nonflotation cushions. This critical curve, or criterion, produces the maximum lumbar load when compared with other nearby cushion properties. A seat cushion replacement methodology was developed and validated, based on these data. This methodology can be used to show that a potential replacement seat cushion produces a greater or lesser lumbar load than a baseline cushion for which lumbar load data have been measured.

The load-deflection data for laminated flotation cushions show a trend that is similar to that shown for the nonflotation cushions. These data are similar to, but more complicated than, the corresponding data for nonflotation cushions. Therefore, additional sled and material test data are required to produce a robust methodology for flotation cushions.

Analyses of the materials data also show that all the cushions exhibit measurable rate sensitivity. Not surprisingly, the dynamic results represent a stronger, stiffer response compared to the static results. The static load-deflection curves for cushions are similar to the dynamic curves, but it is much easier to discriminate between different types of cushions using dynamic data rather than static data. Therefore, it is concluded that dynamic tests at 30 in./sec, such as conducted in this research, are necessary for the seat cushion component test.

6. RECOMMENDATIONS FOR FUTURE RESEARCH.

The use of a validated biodynamic simulation with MADYMO or modified version of SOM-LA to investigate the performance of hypothetical cushions would lead to valuable understanding of the physics governing lumbar load performance. This would be particularly useful in establishing the significance of the unloading curve and the energy absorbed by the cushion on lumbar load. Such a model would facilitate the identification of the criterion curves discussed in this report.

The statistical quality of the data would improve with the inclusion of additional test data. Additional tests are also appropriate to investigate the affects of thickness variations in the BRP region and the lamination of different layers of soft comfort foams. The possibility of placing a limit on how far one is allowed to extrapolate away from the criterion curve should be investigated. This is only an issue for cushions that are stronger than the criterion curve.

Further analytical and experimental studies would contribute to the definition of the criterion curve for laminated flotation cushions. The data set presented in this report are insufficient to quantify the affects of cushion thickness on these curves.

7. REFERENCES.

1. Anon., Title 14 Code of Federal Regulations, Part 25 Airworthiness Standards: Transport Category Airplanes, U.S. Government Printing Office, Superintendent of Documents, Mail Stop SSOP, Washington, D.C. 20402-9328.

2. FAA TSO-C127a, "Rotorcraft, Transport Airplane, and Normal and Utility Airplane Seating Systems," Technical Standard Order, Federal Aviation Administration, Washington, D.C., August 1998.

3. Stech, E.L. and Payne, P.R., "Dynamic Models of the Human Body," Frost Engineering Development Corp., AMRL Technical Report 66-157, Aerospace Medical Research Laboratory, Wright-Patterson Air Force Base, Ohio, November 1969, AD 701383.

4. Anon., *Department of Defense Joint Service Specification Guide - Crew Systems Crash Protection Handbook*, JSSG-2010-7, Wright-Patterson AFB, OH, October 30, 1998.

5. Alfaro-Bou, E., Fasanella, E.L., and Williams, M.S., "Crashworthy Design Considerations for General Aviation Seats," SAE 850855, Society of Automotive Engineers, Warrendale, PA, 1985.

6. Chandler, R.F., "Human Injury Criteria Relative to Civil Aircraft Seat and Restraint Systems," SAE Paper 851847, Society of Automotive Engineers, Warrendale, PA, 1985.

7. SAE AS8049, Rev. A, "Performance Standard for Seats in Civil Rotorcraft and Transport Aircraft, and General Aviation Aircraft," SAE Standard, SAE International, Warrendale, PA, September 1997.

8. Desjardins, S.P., et. al., "Aircraft Crash Survival Design Guide Volume IV – Aircraft Seats, Restraints, Litters, and Cockpit/Cabin Delethalization," Aviation Applied Technology Directorate, USAAVSCOM TR 89-D-22D, U.S. Army Aviation Research and Technology Activity (AVSCOM), Fort Eustis, VA 23604, December 1989.

9. Auyer, W.L., "A Study of the Dynamic Response of a Damped Multi-Degree of Freedom, Spring-Mass System Which Simulates a Seat, Seat Cushion, and Seat Occupant Subjected to a Vertical Impact Acceleration," Thesis, Arizona State University, Tempe, AZ 85287, September 1969.

10. Laananen, D.H. "Computer Simulation of an Aircraft Seat and Occupants(s) in a Crash Environment – Program SOM-LA/SOM-TA User Manual," FAA report DOT/FAA/CT-90/4, May 1991.

11. MADYMO website: http://www.automotive.tno.nl/smartsite.dws?id=1530, September 2004.

12. Coltman, J.W., "Design and Test Criteria for Increased Energy-Absorbing Seat Effectiveness," FAA-AM-83-3. Federal Aviation Administration, Office of Aerospace Medicine, Washington, D.C., 1983.

13. Standard Test Methods for Flexible Cellular Materials-Slab, Bonded, and Molded Urethane Foams, Standard D 3574-03, American Society for Testing and Materials, West Conshohocken, PA 19428-2959, 2003.

14. Gibson, L.J. and Ashby, M.F., *Cellular Solids – Structure and Properties*, second ed., Cambridge University Press, Cambridge, UK, 1997.

15. Anon., Advisory Circular AC 25.562-1A, Dynamic Evaluation of Seat Restraint Systems & Occupant Protection on Transport Airplanes," U.S. Government Printing Office, Superintendent of Documents, Mail Stop SSOP, Washington, D.C. 20402-9328.

16. Bathe, K.J., *Finite Element Procedures*, Prentice-Hall, Englewood Cliffs, New Jersey 07632, 1996.

17. Hosford, W.F. and Caddell, R.M., *Metal Forming- Mechanics and Metallurgy,* 2nd ed., PTR Prentice-Hall, Englewood Cliffs, New Jersey 07632, 1993.

18. Hooper, S.J. and Henderson, M.J., "Development of a Component Test for Crashworthy Seat Bottom Cushions," JBDA Report No. JBDA-01013RR, Final Report: NASA Contract No. NAS1-01013, February 13, 2003.

19. Anon., "Development of a Seat Cushion Replacement Component Test Method for Dynamically Certified Seats," AGATE Report, C-GEN-3433B-1, NASA AGATE Final Report, AGATE Alliance, Inc., Hampton, VA, June 6, 2001.

20. http://www.earsc.com/HOME/products/CushioningMaterials/CONFORFoams/, September 2004.

21. FAA TSO-C72c, "Individual Flotation Devices," Technical Standard Order, Federal Aviation Administration, Washington, D.C., February 1987.

22. DeWeese, R., Personnel Communications, September 2004.

APPENDIX A—DYNAMIC SLED TEST RESULTS

The results of the dynamic seat tests conducted at the Federal Aviation Administration Civil Aerospace Medical Institute in Oklahoma City are summarized in table A-1.

TABLE A-1—SUMMARY OF DYNAMIC SLED TEST RESULTS

Specimen Name	Matl. Spec. No. (NIAR)	Cush. Spec. No. (CAMI)	CAMI Test No. (Sled Test)	Sled Peak G	Pelvis Peak Fz	Pelvis Fz Normalized
NAwa2C450	311	508	A04090	15.2	1948.3	1794.5
NAwa3C200	313	510	A04061	14.3	1896	1856.2
NAwa3C325	315	511	A04065	14.7	1867.6	1778.7
NAwa3C450	317	512	A04069	15.6	2380.9	2136.7
NCwb2C450	329	526	A04086	15	1819.8	1698.5
NDwd1C200	331	528	A04035	13	1089.3	1173.1
NDwd1C325	333	529	A04055	14.7	1259.7	1199.7
NDwd1C450	335	530	A04058	14.7	1316.5	1253.8
NDwd3C200	343	537	A04057	14.9	1311.7	1232.5
NDwd3C325	345	538	A04063	14.6	1222.1	1171.9
NDwd3C450	347	539	A04066	14.7	1213.6	1155.8
FAF1wa1Ct1	351	541	A04093	14.9	1384.3	1300.7
FAF1wa2Ct	355	543	A04052	14.7	1183.7	1127.3
FAF1wa2Ct1	357	545	A04060	14.4	1507.5	1465.6
FAF1wa2Ct3	359	547	A04068	15.1	1973.5	1829.7
FAF1wa3Ct1	363	550	A04091	15	1508.7	1408.1
FAF1wa3Ct3	365	551	A04087	15.2	1912.4	1761.4
FAF2wa2Ct	367	552	A04054	14.7	1237.5	1178.6
FAF2wa2Ct1	369	554	A04059	14.7	1379.6	1313.9
FAF2wa2Ct3	371	556	A04067	15.1	1984.2	1839.7
FAF3wa2Ct3	377	562	A04089	15.1	1979.1	1834.9
FBEwb2Ct	379	567	A04053	14.9	1154.9	1085.1
FBEwb2Ct1	381	569	A04056	14.8	1333.5	1261.4
FBEwb2Ct3	383	571	A04064	14.5	1461.1	1410.7

APPENDIX B—CRITERION CURVE STRESS-STRAIN DATA

The stress-strain data for the criterion curves are provided in this appendix. These data are abbreviated forms of the complete data sets, but provide sufficient precision for most applications. The nonflotation cushion criterion curve is based on the stress-log strain curve presented in figure B-1. These data are also presented in table B-1.
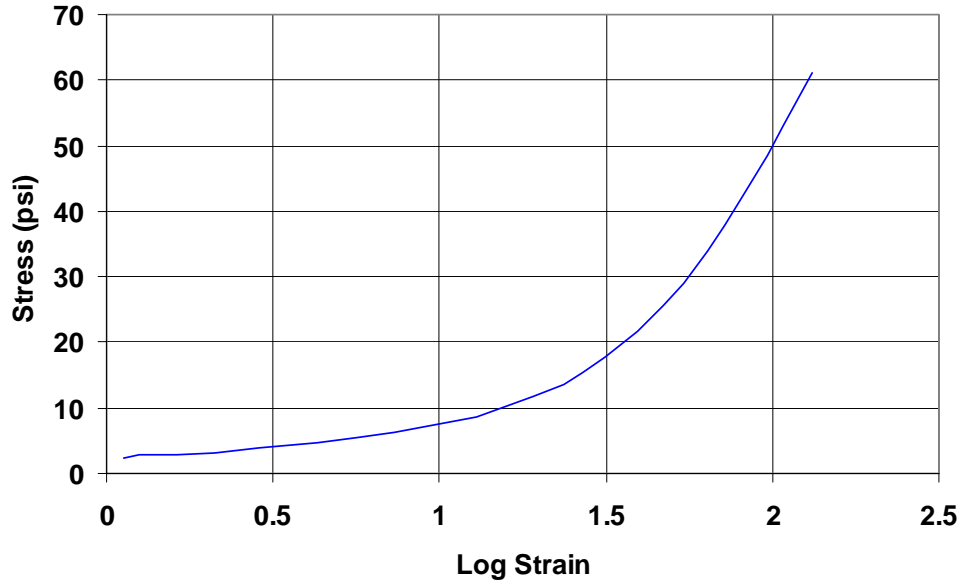

FIGURE B-1. NONFLOTATION CRITERION STRESS-STRAIN CURVE

TABLE B-1. NONFLOTATION CRITERION DATA

Log Strain (ε)	Stress (σ) (psi)
0.05243	2.44
0.09787	2.96
0.20997	2.76
0.32303	3.10
0.45947	3.82
0.63318	4.70
0.75321	5.55
0.86420	6.33
0.97180	7.33
1.11172	8.58
1.28252	11.69
1.37348	13.62
1.43147	15.49
1.49758	17.86
1.59271	21.78
1.66936	25.62
1.73150	29.05
1.80730	34.03
1.85584	37.83
1.91604	42.64
1.98360	48.52
2.03137	53.09
2.12113	61.17